COMPUTER IMPLEMENTATION OF SYMPLECTIC INTEGRATORS AND THEIR APPLICATIONS TO THE N-BODY PROBLEM

by

Rory Michael Casey

A thesis submitted to the faculty of
The University of North Carolina at Charlotte
in partial fulfillment of the requirements
for the degree of Master of Science in
Applied Mathematics

Charlotte

2020

Approved By:

Dr. Xingjie Li

Dr. William Brian

Dr. Hae Oh

ABSTRACT

RORY MICHAEL CASEY. Computer Implementation of Symplectic Integrators and Their Applications to the N-body Problem (Under the Direction of DR. XINGJIE LI)

This research has worked to develop a general computer implementation for symplectic algorithms applied to the N-body problem. A program was written to evolve an arbitrary N-body problem with an arbitrary symplectic integration algorithm so long as the coefficient matrix corresponding to the algorithm is known. After the implementation was completed, a set of sample two and three body systems were evolved using the symplectic integration methods. It was found that high accelerations cause the symplectic algorithms to fail in terms of accuracy. It was also found that while high order integrators struggled to accurately evolve a system with very long time steps, they far surpassed low order methods as the time step was reduced. It was also found that the symplectic integrators were better able to evolve N-body problems over long time intervals than the backward differentiation formula methods.

ACKNOWLEDGEMENTS

I would like to take a moment to give acknowledgement and thanks to several individuals who have been critical to this research. Firstly, I would like to thank Dr. Xingjie Li who has helped me to learn how to perform research in a formal manner. She has also pushed constantly to improve the quality and focus of my research. She has guided my interest in this research and been an important advisor and mentor throughout my career at UNCC, and I would not have completed this research without her assistance. I would also like to thank Dr. Grant Thompson from Wingate University for his constant assistance with this research. Dr. Thompson initially helped me to develop a passion for dark matter research and has helped me to maintain focus on that goal. His interest in my pursuit of research has been an important motivator as I have pursued this work.

TABLE OF CONTENTS

LIST OF TABLES

LIST OF FIGURES

LIST OF ABBREVIATIONS

1. MACHO	Massive Astrophysical Compact Halo Objects
2. WIMP	Weakly Interacting Massive Particles
3. BDF	Backward Differentiation Formulas
4. CEN2	Two Body Centauri
5. SE	Sun-Earth
6. EM	Earth-Moon
7. JI	Jupiter-Io
8. PM2	First Randomly Generated Two Body
9. WR2	Second Randomly Generated Two Body
10. CEN3	Three Body Centauri
11. SEM	Sun-Earth-Moon
12. SEJ	Sun-Earth-Jupiter
13. SJS	Sun-Jupiter-Saturn
14. SMV	Sun-Venus-Mercury
15. WR3	Randomly Generated Three Body

1 INTRODUCTION

In the world of physics, the goal is always to understand that which lies beyond the scope of human knowledge. From the earliest days of history, humanity has tracked the stars, explored the furthest reaches of nature, worked to understand quantum mechanics, and model the mathematics of a black hole's interior. This particular research had the goal of exploring the use, development, and implementation of symplectic integrators in regards to the N-body problem. In the first section, past research on the subject is covered, the history of the N-body problem is explored, and its construction as a Hamiltonian problem is defined to allow the use of symplectic integration techniques. In the second section, the specific symplectic integrators that are used will be introduced. In the third section, a series of example systems are developed to test the four symplectic integration methods over different time steps and for different time intervals. Finally, in the fourth section, the results of the various integrations will be presented and the errors in the systems will be analyzed.

1.1 Previous Research

In previous research, the N-body problem was studied as it relates to the study of dark matter. Dark matter is the enigmatic source of stability in the universe. While dark energy drives space-time itself apart, dark matter holds the universe together. [1] Without dark matter, even the Milky Way galaxy would not survive. Most stars in our galaxy would be cast into deep space and galactic cohesion would be lost. While scientists possess a sound understanding of the importance of dark matter, their understanding of the nature of this phenomenon is minimal at best. It is known that dark matter interacts gravitationally following the laws of general relativity and is approximated by Newtonian mechanics. It is also known that dark matter does not interact electromagnetically or through the strong and weak forces. The universal structure and distribution of dark matter is also known. [1]

Despite understanding specific indirect information regarding dark matter, no one has ever been able to explain what all dark matter is, where it comes from, and how it is distributed on local scales.

As to what dark matter is, it is commonly accepted that there are three possibilities for the nature of dark matter: MACHOs, WIMPs, and neutrinos. [1] MACHOs are large objects like rogue planets, brown dwarfs, black holes, or neutron stars. The objects are difficult to detect which allows them to be considered dark matter. However, it is generally accepted that MACHOs are not the primary candidate for dark matter. [1] If they were, there would be trillions of black holes and other objects stretching in narrow web-like bands between galactic clusters, which is not behavior predicted by the current understanding of physical laws. It is important to remember that while MACHOs may not be the largest contributing factor to dark matter mass, when studying dark matter on local galactic scales, a good model will always account for them because they do exist in the system. WIMPs are the next model commonly used to explain dark matter. WIMPs are derived from supersymmetric extensions to the standard model of particle physics and at this point remain a concept described by theoretical mathematics rather than accepted physics. These particles are essentially super sized versions of common particles such as leptons. [1,2] They are developed as a mathematical solution to known problems with the standard model, but to date, there are no theories about where they come from, how they are produced, how many are expected to exist, or why particles with one thousand times the mass of a proton have never been observed if WIMPs make up 27% of the known universe. [3,4] Neutrinos, on the other hand, are very well understood. First postulated by Wolfgang Pauli to explain nuclear decay, neutrinos are an accepted part of the standard model of particle physics. [2] Neutrinos are commonly made in nuclear fission and fusion reactions including those in stars where hundreds of billions of neutrinos are produced every second by a single star. [2] The only issue with neutrinos being the primary contributor to dark matter is that their

mass is currently unknown. Upper limits have been placed on their mass, but without an exact number, it is difficult to know if they can truly account for as much as twenty-seven percent of the universe's mass.

In previous research, work has been done to show that from a numerical perspective, gravitation is the most relevant source of force when evolving the N-body problem. Influences such as radiation pressure were found to have forces of more than twenty orders of magnitude less than gravitation, making them irrelevant. Using this information, a program was created to estimate the amount of dark matter in a galaxy using the central approximation theorem. The program was written to determine how much mass was needed at the center of an arbitrary galaxy to account for the motion of each star. This procedure is common in orbital mechanics and is used to model systems such as the solar system due to the system being nearly isotropic. However, it was found that the calculations were unstable and resulted in mass estimates with twenty to thirty orders of magnitude difference from star to star. As a result, it was determined that a new approach was needed, providing the grounds for this research.

1.2 The N-body Problem

To begin work on numerical integration of the N-body problem, it is important to first understand the N-body problem. The N-body Problem was first postulated by Isaac Newton during his work on *Philosophiae Naturalis Principa Mathematica*. [1] The N-body problem, generally, is the problem of evolving a system of N bodies interacting with each other through gravitational attraction. The problem is interested in forward and backward time evolutions of the system. [5] At first glance, this may seem to be an easy task; after all, Isaac Newton used only analytic geometry to develop rigorous solutions to a variety of three body problems. [6] However, Newton's solutions could not be generalized. In fact, Newton himself uses his third law, "according to this law, all bodies must attract each other," to describe

the interactions which drive this seemingly simple system to chaos. [6] Every object in the N-body system moves according to the simple differential equations governing motion. [7]

Definition 1.2.1 *Let an object under the influence of gravity from N other bodies exist and be denoted by b_0. Then the trajectory of b_0 is the solution to the system of differential equations*

$$\frac{d\mathbf{x}_{b_0}}{dt} = \mathbf{v}_{b_0}(t)$$

$$\frac{d\mathbf{v}_{b_0}}{dt} = \mathbf{a}_{b_0}(t) = \frac{\mathbf{F}_{b_0}(t)}{m_{b_0}}$$

where $\mathbf{x}_{b_0}(t)$ is the position of b_0 at time t, $\mathbf{v}_{b_0}(t)$ is the velocity of b_0 at time t, $\mathbf{a}_{b_0}(t)$ is the acceleration of b_0 at time t, $\mathbf{F}_{b_0}(t)$ is the net gravitational force acting on b_0 at time t, and m_{b_0} is the mass of b_0.

Given that this is a gravitational system, a definition for the force function can also be stated following the work of Newton in *Principia*.

Definition 1.2.2 *For an object of mass m_0 interacting with N additional bodies through gravity, the net force, $\mathbf{F}_0(t)$, at time t can be defined as*

$$\mathbf{F}_0(t) = \sum_{i=1}^{N} \frac{Gm_0m_i(\mathbf{x}_i(t) - \mathbf{x}_0(t))}{\|\mathbf{x}_i(t) - \mathbf{x}_0(t)\|_2^3}$$

where $G = 6.674x10^{-11}$ is Newton's gravitational constant and the 2-norm is normally defined.

The classic N-body problem is to find the trajectories of bodies in a gravitationally interacting system that is defined by a differential system of equations where each of the N bodies in the system has its motion described by the equations in Definition 1.2.1 with accelerations determined by the force function of Definition 1.2.2. This paper will focus on this classic statement of the N-body problem; however, it is important to note that many

other physical problems are modeled in the same way while changing the equivalence of the acceleration and the definition of the force function. For example, N electrically interacting objects of large mass could be described by replacing gravitational force with the formula for electric attraction and repulsion.

The chaotic nature of this general N-body system is what has impeded progress towards a general solution. In fact, the chaotic nature of the problem has led to the common belief that there does not exist a solution to the N-body problem. [5] A more accurate statement is to say there is no closed form solution to the N-body problem. To see why, the degrees of freedom and available integrals of motion must be examined. For the degrees of freedom, it is necessary to understand what information is needed to solve the problem. When solving the N-body problem, finding the position vector at every point in time is the goal. [6] However, the positions of each body are determined by the velocities at each point in time. [1] The velocity vector and position vector of each body contribute three degrees of freedom each to the problem leading to the following statement.

Theorem 1.2.1 *Let there exist an N-body system governed by gravitational interactions only. Then the degrees of freedom for the N-body evolution is* $6N$.

This theorem is obviously true following from the previous statements. It is possible to reduce the degrees of freedom in the N-body system by making use of the first integrals generated by conservation of energy, conservation of angular momentum, and conservation of linear momentum.

Definition 1.2.3 *A first integral of a system of differential equations is a function which remains constant along any solution of the system. Its value is dependent on the particular solution. The integral is algebraic if it can be solved algebraically for one variable in terms of the others.*

The first six integrals of motion can be derived using the conservation of linear momen-

tum. The conservation of linear momentum is the physical law which states that linear motion in a system is conserved. [7] The conservation of linear momentum is commonly applied in problems such as inelastic collisions, and it is equally sound in the N-body problem. The conservation of linear momentum is equivalent to the sum of forces being 0 in an isolated system. So take $\sum_{j=1}^{N} m_j \ddot{\mathbf{r}}_j = 0$ and integrate the system twice to get $\sum_{j=1}^{N} m_j \mathbf{v}_j = \sum_{j=1}^{N} m_j \mathbf{r}_j = \mathbf{0}$ which provides the first 6 first integrals that are relevant. Each component of these two equations provides one first integral. [8,9] The next three first integrals are obtained from the conservation of angular momentum. From the anticommutativity of the cross product, the angular momentum gives $\sum_{j=1}^{N} m_j(\mathbf{r}_j x \ddot{\mathbf{r}}_j) = 0 = \frac{d}{dt}\sum_{j=1}^{N} m_j(\mathbf{r}_j x \mathbf{v}_j)$. So for some constant c, and by the conservation of angular momentum, $\sum_{j=1}^{N} m_j(\mathbf{r}_j x \mathbf{v}_j) = \mathbf{c}$ which gives three first integrals. [8,9] Then using the conservation of energy, a tenth, and final, first integral can be obtained by defining the potential of the system and converting as $\sum_{j=1}^{N} m_j(\dot{\mathbf{r}}_j \ddot{\mathbf{r}}_j) = \frac{d}{dt}(\frac{1}{2}\sum_{j=1}^{N} m_j \mathbf{v}_j^2) = \sum_{j=1}^{N} \frac{\partial U}{\partial \mathbf{r}_j}\mathbf{r}_j = \frac{d}{dt}U$. This gives the equivalence $T = \frac{1}{2}\sum_{j=1}^{N} m_j v_j^2 = U + h$ for some constant h with respect to time. [8,9] These ten first integrals are used to reduce the degrees of freedom of the N-body problem and can be used to show that the two body problem in three dimensions is equivalent to a specially constructed one body problem in one dimension. [5] Unfortunately, for $N \geq 3$, no such reduction is possible. In his work on the three body problem, Poincare proved the following Theorem: [10]

Theorem 1.2.2 *There are no first integrals, algebraic with respect to the time, position, and the velocities only, other than the ten abvove.*

Since the N-body problem has $6N$ degrees of freedom and there are only ten first integrals of motion, the most the system can be reduced is to $6N - 10$ degrees of freedom. For the two body problem, this gives two degrees of freedom which is the one body problem in one dimension as discussed earlier. The general two body solution known as Binet's orbital equation can be derived through complex analysis and is easily followed in the work by

D' Eliseo. [11] For the three body problem, however, the reduction gives eight degrees of freedom, which is why there is no closed form solution for the general N-body problem. Despite having no general closed form solution for the N-body problem, there is a convergent series solution derived by Sundman in [12] for the three body problem in 1913 and extended to the N-body problem by Qiu-Dong in 1990. [13]

For the statements and proofs of the Sundman and Qiu-Dong series solutions to the N-body problem, the reader is referred to the original papers published on the topic. [12,13] It is important to note, however, that the general series solution to the N-body problem presented by Qiu-Dong does not extend to all cases. In Sundman's original work, he analytically extended past binary collisions by recognizing they were algebraic branch points and using a conformal mapping to regularize the phase space. [8,12,14] However, as noted by Qiu-Dong, regularization can only be applied to binary collisions, and it is well known that while the three body problem only undergoes singularity at a binary collision, an arbitrary N-body problem can experience singularities at triple or greater collisions and can even experience singularities at times where there are no collisions. [13] Fortunately, though, it is commonplace to simply ignore initial conditions which result in singularity. This is accepted in the physics community because it has been proven that the set of all initial conditions corresponding to singularity in the N-body problem has Lesbesgue measure zero. [15,16] This theorem is proven clearly in the work by Saari and the reader is referred to that work for a detailed proof.

Theorem 1.2.3 *The set of initial conditions leading to collision in finite time has Lesbesgue measure zero.*

This theorem leads the physics community to accept the Sundman and Qiu-Dong series' as solutions to the three body and N-body problems. However, the work by both of these figures remains fairly unknown because the convergence of the series' is extremely slow. This slow convergence means that, under certain assumptions, a solution to the N-body problem

has been found, but is ultimately not useful because of slow convergence. Therefore, it is important to continue to improve and analyze numerical methods for integrating the N-body problem.

The final theoretical consideration for dynamic systems, like the N-body problem, being evolved in this research is a topic known as attractors. Attractors are an important consideration in dynamic systems because they control the evolution in a dynamic system for long time simulations.

Definition 1.2.4 *Let t be time and $f(t,\cdot)$ be a dynamic function defining the evolution of the system. Then an attractor is a subset, A, of phase space characterized by*

1. *A is forward invariant under f. This means that if $a \in A$, then $f(t,a) \in A$ for all $t > 0$.*

2. *A has a basin of attraction. The basin $B(A)$ is the set of all b in the phase space such that for any open neighborhood N of A, there exists a positive constant T such that $f(t,b) \in N$ for all $t > T$.*

3. *There is no proper, non-empty subset of A with the first two properties satisfied. [17,18]*

There are many kinds of attractors including fixed point attractors, periodic attractors, and strange attractors. In N-body simulations, periodic attractors and strange attractors are the most common types. [18]

Definition 1.2.5 *Let A be an attractor in a dynamic system. Then A is a strange attractor if its structure is fractal in nature. [19]*

Definition 1.2.6 *Let A be an attractor in a dynamic system. Also let $x(t)$ be a closed trajectory in phase space satisfying the differential system being examined. Then A is a limit cycle of the dynamic system if it is the limit set of some trajectory which is not its own.*

These attractors are useful in N-body systems because most real N-body systems are stable systems that destroy or merge together bodies that would drive the system to chaos. For example, the Sol system once had a planet between Earth and Mars that was obliterated in a collision which led to a more stable system and the Earth's moon. [1] In large N-body systems where all bodies have regular orbits, periodic attractors will pull nearby trajectories to themselves as time proceeds to infinity even if the trajectory is slightly disturbed. In the symplectic integration techniques that will be used for this research, the error at each time step appears mathematically as a slight disturbance in the trajectory away from a body's true orbit. This means that when combined with 2-form conservation that will be discussed later, the presence of periodic attractors in the N-body system guarantee long term stability of symplectic integration. To locate these special features of dynamic systems, Lyapunov functions are commonly used. While a detailed description of the many applications of Lyapunov functions is beyond this paper, the reader is referred to [20] for examples of and uses of Lyapunov functions in locating attractors for dynamic systems.

1.3 Hamiltonian Mechanics

While studying the N-body problem, the second step is in understanding the way in which it is viewed by mathematicians and physicists today. To do this, it is important to understand the basics of Hamiltonian mechanics.

Definition 1.3.1 *A Hamiltonian system is a dynamic system of differential equations defined by:*

$$\frac{dp}{dt} = -\nabla_q H(p,q)$$

$$\frac{dq}{dt} = \nabla_p H(p,q)$$

where p is the momentum in phase space, q is the position in phase space, and H is the Hamiltonian function of the system. [21]

For many general mechanics problems, including the N-body problem, the Hamiltonian is representative of the total energy of the system and is therefore separable. [22]

Definition 1.3.2 *Let $K(p)$ be the kinetic energy of an N-body system, and let $U(q)$ be the potential energy of the system. Then the separable Hamiltonian, H, of the N-body system is [23]*

$$H(p,q) = K(p) + U(q)$$

For a specific example on constructing the Hamiltonian of a system, the reader is referred to [24] which constructs the Hamiltonian for triaxial galactic nuclei.

Hamiltonian systems are important to the understanding of the N-body problem because they possess several important properties. The first of these properties is the simplicity of the 2-form in phase space. The 2-form of the Hamiltonian system is [21] $H(p,q)dp \wedge dq$ with the relevant integral being

$$\int_S H(p,q)dp \wedge dq$$

When discussion begins on symplectic integrators in a later section, the 2-form becomes a very important property of the Hamiltonian system. [23,25] For now, it is sufficient to know that this 2-form defines the differential form, or geometry, of the phase space related to the Hamiltonian. [21] In addition to the 2-form, Hamiltonian systems are useful in studying the N-body problem because they are well known producers of attractors which are important in ensuring convergence of a dynamic system. Understanding the N-body problem as a Hamiltonian problem is also relevant to this research because symplectic integrators are specifically designed to work on Hamiltonian systems. [26] They cannot be used, in general, for non-Hamiltonian systems.

2 INTEGRATION TECHNIQUES

The next important topic to cover in research regarding the symplectic integrators is the integrators themselves. In the following sections, the backward differentiation formulas will be presented first. These methods are well understood and Python has existing packaging to make use of a 6th order BDF method which will allow for accurate short time evolution of each system. The short time evolution of each system will serve as a reference system to compare the symplectic integrators to with a variety of time steps. Following the BDF method explanations, a basic example of long time error in BDF method evolution will be examined in the classic explicit Euler method. After it becomes clear that long time simulation of the N-body problem requires a more accurate numerical approach than the BDF methods, the four symplectic integrators that will be used here are the first order symplectic Euler method which is a slight modification of the explicit Euler method, the second order Verlet method which is closely related to the traditional leap-frog algorithm, the third order Ruth method, and the fourth order Neri method.

2.1 Backward Differentiation Formulas

The first group of integration techniques that will be examined here are the BDF methods. BDF methods are a class of integrators designed for use in stiff systems of ordinary differential equations such as the N-body problem. [27] The classic explicit Euler method is the first order BDF method. This shows the primary strength and weaknesses of this class of integrators. The main strength of these schemes is their ease of implementation. This strength is offset by lack of accuracy. As with any numerical scheme, the BDF methods rely on mesh size to become accurate; the shorter the time step at each approximation, the better the estimate that is returned. [28] The sixth order BDF method used to generate the reference systems in this research will rely on a mesh size of $\Delta t = 0.0016$. As will be discussed in the results section later, even over the short-time intervals that will

be examined in this research, the accumulating error of the BDF methods is evident. As $t \to \infty$ a BDF method will always eventually diverge from the true solution no matter the mesh size. [28] The need to constantly reduce mesh size with increasing time makes BDF methods inappropriate for long-time evolution of an N-body system. The 6th order BDF method used for the short-time reference systems in this research is appropriate because of the short-time intervals. However, an N-body system that needs to evolve over millions of years (such as a galaxy) would be an inappropriate use of a BDF method. The general algorithm for a multi-step method is: [27,28,29]

$$\sum_{i=0}^{k} \alpha_{k-i} u_{n+1-i} - h_n \sum_{i=0}^{k} \beta_{k-i} f(t_{n+1-i}, u_{n+1-i}) = 0$$

This is adapted for the BDF methods to:

$$\sum_{i=1}^{k} \frac{1}{i} \nabla^i u_{n+1} = h f(t_{n+1}, u_{n+1}) + u_{n+1}$$

For example, the 3rd order BDF method is:

$$u_{n+1} = \frac{18}{11} u_n - \frac{9}{11} u_{n-1} + \frac{2}{11} u_{n-2} + \frac{6h}{11} f(t_{n+1}, u_{n+1})$$

2.2 Explicit Euler Example

As an example of the failures of BDF methods, a simple example of the class explicit Euler method will be presented here. This simple method can be formally stated as [28]

$$u_{n+1} = u_n + h f(t_n, u_n)$$

For this example take the initial value problem $y' = y, y(0) = 1$ which has the true solution $y = e^t$. The explicit Euler method for $\Delta t = 1.0$ and $\Delta t = 0.25$ are given by

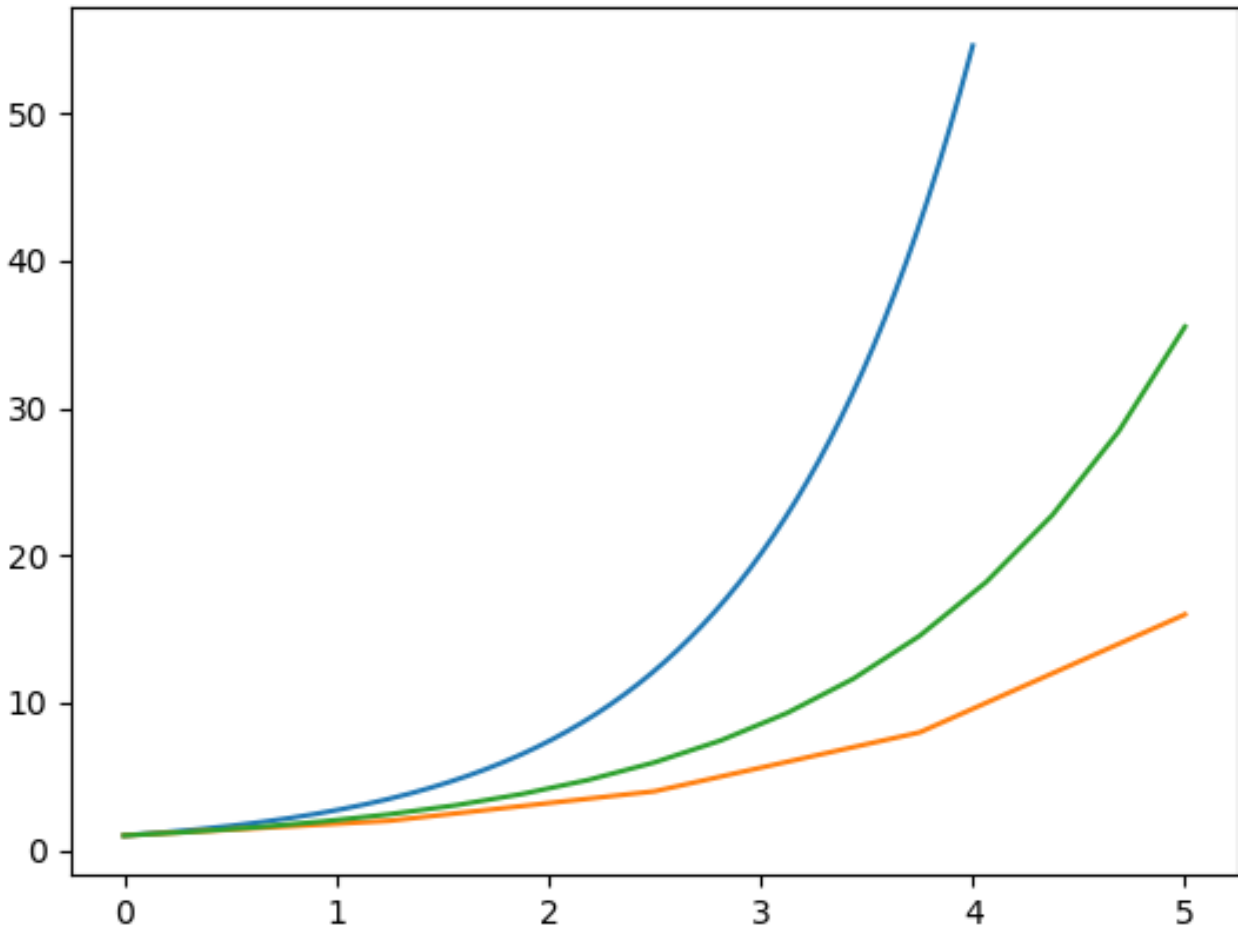

Figure 1: This figure shows the error of the explicit Euler scheme using $\Delta t = 1.0$ and $\Delta t = 0.25$

From this figure, it should be clear that for large mesh size, the explicit Euler method diverges from the true solution rapidly. Also, it should be clear that despite the smaller mesh size, the Explicit Euler method still eventually diverges from the true solution. This long-time divergence from the true solution of the problem is a feature shared by all BDF methods. [28]

2.3 Symplectic Integrators

This section will discuss the Symplectic schemes that will be used to evolve systems for this research. Before beginning a discussion of each independent scheme, some time should

be devoted to discussing what it means for an integrator to be symplectic, the properties of these integrators, and why they are so important to Hamiltonian systems like the N-body problem.

Definition 2.3.1 *An integrator ϕ is symplectic if the trajectory of $\phi(p, q)$ in phase space conserves the 2-form of the Hamiltonian system in phase space. [25]*

Definition 2.3.2 *The two form for an arbitrary Hamiltonian system, including the N-body problem, is given by $H(p, q)dq \wedge dp$ and has the integral $\int_S H(p, q)dq \wedge dp$. [21]*

Any integrator which conserves this 2-form in phase space is a symplectic integrator. [21,25] It is important here to understand what it means to conserve the 2-form in phase space. The 2-form in phase space defines the global interactions of the momentum and position components of the Hamiltonian. Since the 2-form defines area in this phase space, the integral $\int_S H(p, q)dp \wedge dq$ defines the total energy of the system. Therefore, a symplectic integrator will conserve the total energy of the system. [21] This is an important distinction from energy conservative integrators. Conserving the total energy of the system offers no guarantees on the individual energies associated with each body. For example, if the area in phase space is a rectangle with width 2 and length 1, then the energy is 2. Under a symplectic map, we expect this 2 to be conserved, but we cannot guarantee that the new shape is a rectangle at all. In the N-body problem, this means we expect the total sum of the kinetic and potential energy to be conserved, but the symplectic map offers no guarantee that every star will adhere to its true orbit.

While the nature of a symplectic transform itself offers no guarantee about adherence of individual bodies to their true orbits, a special property of the N-body system does. As discussed earlier, in most naturally occurring N-body systems, objects orbit in regular elliptical patterns which allows attractors in the system to be considered. The most common types of attractors are strange attractors which are prominent in systems like the Lorenz-63

system, periodic attractors which are prominent in systems like dual pendulum motion, and fixed point attractors.

Definition 2.3.3 *Let σ, ρ, and β be physical constants defining an atmospheric system. Then the Lorenz-63 system is given by: [30]*

$$\frac{dx}{dt} = \sigma(y - x)$$

$$\frac{dy}{dt} = x(\rho - z) - y$$

$$\frac{dz}{dt} = xy - \beta z$$

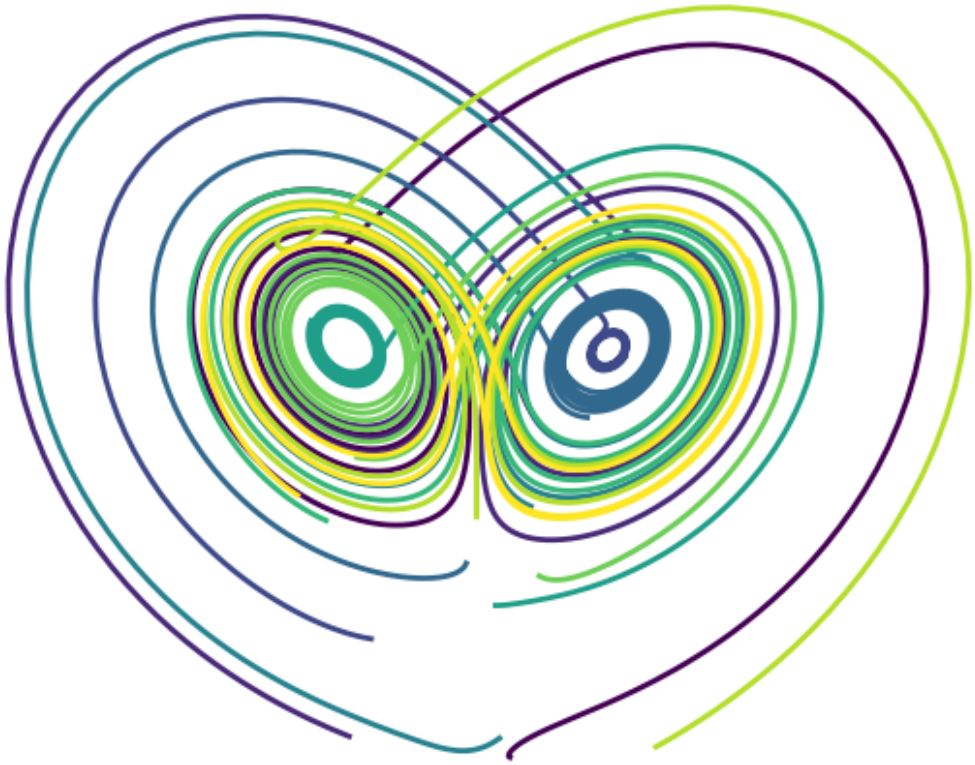

Figure 2: This image gives a sample Lorenz-63 system.

For some initial conditions, a single fixed point attractor is present resting just outside the butterfly loop. For some initial conditions, two strange attractors are present in the center of the loop. Still other initial conditions can result in a system which decays into random motion and does not have an attractor. The N-body system for certain initial conditions can contain strange attractors, periodic attractors, both, or neither, making it somewhat more complex of a case study. However, the regular orbits of realistic N-body gravitational systems mean that periodic attractors can be both common and useful. The presence of periodic attractors in the phase space of realistic N-body problems provides that once stars approach their true orbits in simulation, they will not seriously diverge for a symplectic integrator. For example, when evolving the Sun-Earth-Moon system, you might

expect the Earth to occasionally be outside or inside its true orbit, but the nature of the attractor means that it will always return to its true path.

There are many forms of symplectic integrators, some of which are designed to be symplectic and some of which just happen to be when applied to a Hamiltonian problem. One group of methods which just happens to be symplectic are the Runge-Kutta methods. The 4 methods this research will focus on–Symplectic Euler, Verlet, Ruth, and Neri–are all examples of integrators that are constructed to be symplectic. They are specifically designed to be used for Hamiltonian systems. In general, all designed symplectic integrators are a symplectic transformation on the initial conditions called a symplectic mapping. [21] This mapping can be simply written as $(p_{n+1}, q_{n+1}) = \phi_{t,H}(p_n, q_n)$. The symplectic integration methods are all examples of the $\phi_{t,h}$ function. They take the system from a given point to the next unknown point. Before studying each scheme in detail, we should look at how these schemes are generally developed.

Let A and B be non-commutative operators and τ be a small real number. Then the goal of developing a symplectic integrator is to find 2 sets of real numbers $(c_1, c_2, ..., c_k)$ and $(d_1, d_2, ..., d_k)$ such that the following equality holds for a given positive integer n,[26]

$$e^{\tau(A+B)} = \prod_{i=1}^{k} e^{c_i \tau A} e^{d_i \tau B} + o(\tau^{n+})$$

To derive this formula, we look at the methods used by Neri in [31]. First rewrite the Hamiltonian equations in the form $\frac{dz}{dt} = \{z, H(z)\}$ where the Poisson bracket $\{z, H(z)\}$ is defined by the form $\{F, G\} = F_q G_p - F_p G_q$. Then define D_G to be a differential operator by $D_G F := \{F, G\}$. Then the Hamiltonian system can be written as $\epsilon = D_H z$. Then we get the time evolution of $z(t)$ from $t = 0$ to $t = \tau$ by $z(\tau) = z(0)e^{\tau D_H}$. For a separable Hamiltonian like the N-body problem, this becomes $z(\tau) = z(0)e^{\tau(A+B)}$ where $A := D_K$ and $B := D_U$. Then for two sets of numbers $(c_1, c_2, ..., c_k)$ and $(d_1, d_2, ..., d_k)$ satisfying

$z(\tau) = z\{\prod_{i=1}^{k} e^{c_i \tau A} e^{d_i \tau B}\}$ the integrators defined by the sets $(c_1, c_2, ..., c_k)$ and $(d_1, d_2, ..., d_k)$ are symplectic because they are the product of elementary symplectic maps.[21,26] The coefficients c_i and d_i in this case will be chosen to compel $z(\tau)$ to correspond with the Taylor expansion of the true solution to order τ^n. For this research, methods of this form will be used. However, as noted by Yoshida in [26] higher order symplectic integrators can be generated for even order from these methods. Let $S_2(\tau) := e^{\frac{\tau}{2}A} e^{\tau B} e^{\frac{\tau}{2}A}$. Then it is clear that this corresponds to the Verlet method. Then higher order integrators can be found by

$$S_n(\tau) = S_2(\omega_n \tau) S_2(\omega_{n-1} \tau) ... S_2(\omega_1 \tau) S_2(\omega_0 \tau) S_2(\omega_1 \tau) ... S_2(\omega_{n-1} \tau) S_2(\omega_n \tau)$$

It should be noted that these integrators are computationally difficult to find for order $n \geq 6$. It should also be noted that the general form for an algorithm using these coefficients for time step dt is given by [32]

$$v^{(i)} = v^{(i-1)} + c_i a(x^{(i-1)}) dt$$

$$x^{(i)} = x^{i-1} + d_i v^{(i)} dt$$

for $i = 1, 2, ..., I$. Here the (i) labels denote the particular intermediate step where there are I steps total in the algorithm.

2.3.1 First Order Symplectic Euler Method

The first symplectic integration technique introduced for this research is the symplectic Euler method. It is a slight modification on the classic explicit Euler method that updates velocities before updating positions. Following the derivations presented in the introduction to this section, the symplectic Euler method can be defined as a trivial solution to the satisfying Neri's constructions.

Definition 2.3.4 *Let C be a matrix holding values corresponding to the coefficients that solve the system of equations constructed in the previous system. Let the first row hold values for c_i and the second row hold values for d_i. Then the symplectic Euler method is defined by [23]*

$$\mathbf{C} = \begin{bmatrix} 1 \\ 1 \end{bmatrix}$$

This equates to the system of ordered equations for step size dt

$$v_{n+1} = v_n + a_n dt$$

$$x_{n+1} = x_n + v_{n+1} dt$$

where x_n, v_n, and a_n correspond to the position, velocity and acceleration at time $t = n$ and x_{n+1}, v_{n+1} correspond to the position and velocity at time $t = n + 1$. This method is primarily used as a fast integration method for systems that do not experience extreme instabilities. It is also useful in determining the process that needs to be undertaken to implement a general method for symplectic integration.

2.3.2 Second Order Verlet Method

The second symplectic integration technique introduced for this research is the second order Verlet method. It is a technique very closely related to the leapfrog algorithm. [28] In the classic leapfrog algorithm, the velocity is updated to a half time step ahead of the position for the body. Then in a similar manner to the symplectic Euler method, the positions and velocities are updated in sequence. The leapfrog algorithm gives a multi-step method described by the equations [33]

$$x_{n+1} = x_n + v_{n+1/2} dt$$

$$v_{n+3/2} = v_{n+1/2} + a(x_{n+1})dt$$

The symplectic single step Verlet method differs slightly. Rather than updating the velocity to half time step, the update on the velocity is split into two portions. The velocity is updated, then the position is updated, and the velocity is then updated a second time. This algorithm corresponds to a single time step leapfrog algorithm. Following the work from the previous sections, the Verlet method can be seen as the second order scheme that is used to construct the higher order symplectic integrators.

Definition 2.3.5 *Let C be constructed similarly to the symplectic Euler method. Then the Verlet method is defined by [33]*

$$\mathbf{C} = \begin{bmatrix} \frac{1}{2} & \frac{1}{2} \\ 1 & 0 \end{bmatrix}$$

This method equates to a system of ordered equations for step size dt

$$v_{n+\frac{1}{2}} = v_n + \frac{1}{2}a_n dt$$

$$x_{n+1} = x_n + v_{n+\frac{1}{2}}dt$$

$$v_{n+1} = v_{n+\frac{1}{2}} + \frac{1}{2}a_{n+1}dt$$

In general symplectic integration, the velocity and position would be updated the same number of times. However, in the Verlet method, the second update of position has a coefficient of zero which is equivalent to not updating the position a second time. The Verlet method is commonly used in evolutions of N-body problems and was the commonly accepted method prior to development of higher order symplectic algorithms. [34] When implementing a general method for arbitrary symplectic integration, it is also useful for testing the code for errors in iterating over the list of coefficients. Once the process for the symplectic Euler and Verlet methods is understood, implementing other symplectic

integrators is simple.

2.3.3 Third Order Ruth Method

The third symplectic integration technique to be covered for this research is the third order Ruth method. It is a scheme that was originally developed for use in dynamic chemical reactions and seismology. The Ruth method is the first symplectic algorithm that will fully test the general implementation of an arbitrary symplectic scheme. It has all non-zero coefficients which corresponds to evolving the velocity and position three times each.

Definition 2.3.6 *Let C be constructed similarly to the previous sections. Then the Ruth method is defined by [35]*

$$\mathbf{C} = \begin{bmatrix} \frac{7}{24} & \frac{3}{4} & \frac{-1}{24} \\ \frac{2}{3} & \frac{-2}{3} & 1 \end{bmatrix}$$

This scheme is the most commonly used 3rd order symplectic scheme and is described by the equations, [35]

$$v^{(1)} = v^{(0)} + c_1 a(x^{(0)})dt$$

$$x^{(1)} = x^{(0)} + d_1 v^{(1)} dt$$

$$v^{(2)} = v^{(1)} + c_2 a(x^{(1)})dt$$

$$x^{(2)} = x^{(1)} + d_2 v^{(2)} dt$$

$$v^{(3)} = v^{(2)} + c_3 a(x^{(2)})dt$$

$$x^{(3)} = x^{(2)} + d_3 v^{(3)} dt$$

2.3.4 Fourth Order Neri Method

The final symplectic integration technique introduced for this research is the fourth order Neri method. Originially developed by Neri for use in research done by particle accelerators,

the Neri method is the most robust algorithm used for this research. It updates velocity and position four times each and does a series of forward and backward steps in time to get the best approximation for the value at the computed time step.

Definition 2.3.7 *Let C be constructed similarly to the previous sections. Then the Neri method is defined by [31]*

$$\mathbf{C} = \begin{bmatrix} \frac{1}{2(2-2^{1/3})} & \frac{1-2^{1/3}}{2(2-2^{1/3})} & \frac{1-2^{1/3}}{2(2-2^{1/3})} & \frac{1}{2(2-2^{1/3})} \\ \frac{1}{2-2^{1/3}} & \frac{-2^{1/3}}{2-2^{1/3}} & \frac{1}{2-2^{1/3}} & 0 \end{bmatrix}$$

The ordered equations for the Neri method are the most accurate of the symplectic algorithms for this research, but as will be seen in later portions of this work, often require shorter time steps to function properly. The ordered equations for the Neri method are [31]

$$v^{(1)} = v^{(0)} + c_1 a(x^{(0)})dt$$

$$x^{(1)} = x^{(0)} + d_1 v^{(1)} dt$$

$$v^{(2)} = v^{(1)} + c_2 a(x^{(1)})dt$$

$$x^{(2)} = x^{(1)} + d_2 v^{(2)} dt$$

$$v^{(3)} = v^{(2)} + c_3 a(x^{(2)})dt$$

$$x^{(3)} = x^{(2)} + d_3 v^{(3)} dt$$

$$v^{(4)} = v^{(3)} + c_4 a(x^{(3)})dt$$

$$x^{(4)} = x^{(3)} + d_4 v^{(4)} dt$$

3 CONSTRUCTION OF THE SAMPLE SYSTEMS

Now that the necessary background of the N-body problem, its structure as a Hamiltonian problem, and specific integration techniques have been covered, it is necessary to construct a series of sample systems to test the symplectic integrators that were developed in the previous section. For the purposes of testing the integrators, a series of two and three body problems will be used. The problems will have a variety of initial conditions and scaling factors to force the system to unity and decrease computational load. The systems will display normal elliptical orbits, rapidly spiraling orbits, and far more chaotic behavior for some three body examples. The predictable behavior of the two body systems make them good systems to train an integrator against while the chaotic behavior of the three body systems will allow the integrators to be stressed sufficiently to determine circumstances which causes them to fail.

Before constructing the systems, it is important to develop the scaled differential equations that will actually be approximated by the integrators. The scaling of these systems is pursued by removing the dimensions of the differential equations. Previously, it was stated that the Hamiltonian form of the differential equations for motion

$$\frac{d\mathbf{x}(t)}{dt} = \mathbf{v}(t)$$

$$\frac{d\mathbf{v}(t)}{dt} = \frac{\mathbf{F}(t)}{m}$$

can be used to evolve these systems. Then an equivalent unity system can be constructed according to the following definition.

Definition 3.0.1 *Let the Hamiltonian system be defined as previously stated in Definition 1.2.1. Then define m_{ref} to be a reference mass for a system, r_{ref} to be a reference distance for a system, v_{ref} to be a reference velocity for a system, and t_{ref} to be a reference time for*

a system. Then define

$$K_1 = \frac{Gt_{ref}m_{ref}}{v_{ref}r_{ref}^2}$$

$$K_2 = \frac{v_{ref}t_{ref}}{r_{ref}}$$

Then the system defined by

$$\frac{\bar{\mathbf{x}}(t)}{dt} = K_2\bar{\mathbf{v}}(t)$$

$$\frac{\bar{\mathbf{v}}(t)}{dt} = K_1\frac{\bar{\mathbf{F}}(t)}{m}$$

evolves in a reference space defined by reference units with trajectories equivalent to the original system.

3.1 Construction of the Two Body Systems

In this section, the initial conditions of the two body systems, their scaling variables, and the expected behavior of the systems will be presented. As discussed in the previous section on the N-body problem, these systems have an analytic solution that is equivalent to a one body problem with initial conditions based on the initial conditions of the two body problem. Because of this, their behavior is easily predicted. The predictable behavior makes these systems strong test systems. Numerical integration techniques can be trained against the known solutions for two body systems to test for appropriate step sizes to approximate the solution of a system. All values for systems presented in this section except for the randomly generated systems can be found in [1].

3.1.1 Two Body Centauri System

The first two body problem that will be considered is the core system of the Centauri star system. The Centauri star system is a trinary system with two dominating masses and a third, much smaller star. The two dominating masses spiral around each other

and translate slowly down a central axis. This behavior makes this system an important step for each integrator. It displays translation and rotation behavior which provides two different types of motion for the integrator to track offering a greater challenge than one behavior or the other. As a phase one tester, all four integrators will accurately evolve this system with an appropriate time step. The two body Centauri system will use the following reference variables for scaling: $m_{ref} = 1.989x10^{30}$, $r_{ref} = 5.326x10^{12}$, $v_{ref} = 3.0x10^{4}$, and $t_{ref} = 1.285x10^{9}$. In reference units, the initial conditions of this system are:

$$X = \begin{bmatrix} -0.5 & 0 & 0 \\ 0.5 & 0 & 0 \end{bmatrix}$$

$$V = \begin{bmatrix} 0.01 & 0.01 & 0 \\ -0.05 & 0 & -0.1 \end{bmatrix}$$

$$M = \begin{bmatrix} 1.1 \\ 0.907 \end{bmatrix}$$

Here, X is the initial position matrix, V is the initial velocity matrix, and M is the mass matrix where each row corresponds to a different object.

3.1.2 Sun-Earth-System

The second two body problem which will be used to train the integrators is the Sun-Earth system. This system is a familiar elliptical orbital system which evolves on a plane through the center of the solar system. This system is a significant trial because it has the largest differential in initial conditions for the two body problems. The difference between the masses of the two bodies in this system is six orders of magnitude which assists in determining what initial condition difference can be handled by symplectic integrators before experiencing underflow. In this system, we expect a constant elliptical orbit of the smaller

body about the larger body that evolves on the same plane. This means the Sun-Earth system is challenging only due to its large differential in initial conditions, not due to multiple behaviors being tracked simultaneously. This two body system will use these reference variables for scaling: $m_{ref} = 1.989x10^{30}$, $r_{ref} = 1.486x10^{11}$, $v_{ref} = 3.0x10^{4}$, and $t_{ref} = 3.15576x10^{7}$. In reference units, the initial conditions of this system are given by:

$$X = \begin{bmatrix} 0 & 0 & 0 \\ 1 & 0 & 0 \end{bmatrix}$$

$$V = \begin{bmatrix} 0 & 0 & 0 \\ 0 & 0.99074 & 0 \end{bmatrix}$$

$$M = \begin{bmatrix} 1 \\ 0.0000030025 \end{bmatrix}$$

3.1.3 Earth-Moon System

The third two body system that will be examined here is the Earth-Moon system. This system possesses identical behavior to the Sun-Earth system discussed previously, but it has a much smaller difference in scaled masses of the system. The similarity in masses in this system will mean that the larger body, the Earth in this case, will also exhibit rotational behavior. That difference from the Sun-Earth system makes the Earth-Moon system a significant trial for this research. This system will make use of the following scaling variables: $m_{ref} = 5.972x10^{24}$, $r_{ref} = 3.844x10^{8}$, $v_{ref} = 1.023x10^{4}$, and $t_{ref} = 2.2384x10^{6}$. In reference units, the initial conditions of this system will be given by:

$$X = \begin{bmatrix} 0 & 0 & 0 \\ 0 & 1 & 0 \end{bmatrix}$$

$$V = \begin{bmatrix} 0 & 0 & 0 \\ -1 & 0 & 0 \end{bmatrix}$$

$$M = \begin{bmatrix} 1 \\ 0.012304 \end{bmatrix}$$

3.1.4 Jupiter-Io System

The next system to be examined is the Jupiter-Io system. This system is another large and small body system that lies in between the Sun-Earth system and the Earth-Moon system. As such, it will exhibit a similar rotational system for Io as the Earth or Moon in the two previous systems. However, it will exhibit only minor motion on Jupiter making it more similar to the Sun-Earth system. This allows for examining what order of magnitude difference in masses leads the integrator to zero motion on the primary body. This system will make use of the following scale variables: $m_{ref} = 1.898x10^{27}$, $r_{ref} = 4.217x10^{8}$, $v_{ref} = 1.7334x10^{4}$, and $t_{ref} = 1.52853x10^{6}$. In reference units, the initial conditions are given by:

$$X = \begin{bmatrix} 0 & 0 & 0 \\ 0 & 0 & -1 \end{bmatrix}$$

$$V = \begin{bmatrix} 0 & 0 & 0 \\ 0 & 1 & 0 \end{bmatrix}$$

$$M = \begin{bmatrix} 1 \\ 0.00004706 \end{bmatrix}$$

3.1.5 First Randomly Generated Two Body System

The next system that will be examined is the first of two randomly generated two body systems, each of which displays unique behavior. This system has two bodies of similar

mass positioned equidistant on either side of the origin of the system. The bodies have two different velocities with the largest contribution in the x-direction for one and the z-direction for the other. As such, this system is expected to display oscillatory behavior in both bodies moving through the x-direction and down the z-direction. This system uses scaling variables: $m_{ref} = 8.172x10^{32}$, $r_{ref} = 5.1x10^{9}$, $v_{ref} = 2.512x10^{6}$, and $t_{ref} = 1.75x10^{4}$. In reference units, the initial conditions of this system are:

$$X = \begin{bmatrix} -0.5 & -0.5 & -0.5 \\ 0.5 & 0.5 & 0.5 \end{bmatrix}$$

$$V = \begin{bmatrix} 1.1 & 0 & 0.01 \\ 0.1 & 0.2 & -0.3 \end{bmatrix}$$

$$M = \begin{bmatrix} 1 \\ 1.112 \end{bmatrix}$$

3.1.6 Second Randomly Generated Two Body System

The final two body system that will be examined here is another randomly generated two body system. Rather than displaying an elongated oscillating behavior as in the previous system, this system will be expected to display behavior similar to that of the two body Centauri system. The key difference between the two is the magnitude of the initial velocities. The initial velocities for the two body Centauri system were relatively small. The velocities for this system are between two and four times larger. As a result, this system will experience much sharper orbits and will complete more rotations in the same time interval. This system uses the following reference variables: $m_{ref} = 1.989x10^{31}$, $r_{ref} = 1.123x10^{10}$, $v_{ref} = 6.0x10^{5}$, and $t_{ref} = 6.876x10^{4}$. In reference units, the initial conditions of the system

are given by:

$$X = \begin{bmatrix} 0.5 & 0 & 0 \\ 0 & 0 & 0.5 \end{bmatrix}$$

$$V = \begin{bmatrix} 0.09 & 0.1 & 0.2 \\ -0.09 & -0.1 & -0.2 \end{bmatrix}$$

$$M = \begin{bmatrix} 1 \\ 0.967 \end{bmatrix}$$

The expected behaviors of all the two body systems are summarized in the following table.

Table 1: This table gives a summary of the expected behaviors for the given 2 body systems.

System	Expected Behavior
2 Body Centauri	Orbits Down a Central Axis
Sun-Earth	Regular Elliptical Orbits
Earth-Moon	Regular Elliptical Orbit Around a Wobbling Central Body
Jupiter-Io	Regular Elliptical Orbit
Random 1	Oscillating Pattern
Random 2	Rapid Elliptical Orbit

3.2 Construction of the Three Body Systems

In this section, the initial conditions, scaling variables, and expected behavior for the three body systems will be presented. As discussed in previous sections, the three body problem is the most basic N-body problem which has no general closed form solution. As a result, the expected behaviors of these systems will often be extremely chaotic as will be seen by even the first example–the three body Centauri system. While not as easily predicted as the two body problem, the 6th order backward differentiation formula method used to get the reference systems for the two body problems will still suffice here. These three body problem examples and their varied behavior are a much better test of the symplectic

integrators than the two body problems. While good approximations for the true solution are expected for the two body problems, the three body problems offer an opportunity to stress the integrators and test their usefulness in evolving N-body problems. Similarly to the two body problems, the values for the real systems included here can be found in [1].

3.2.1 Three Body Centauri System

The first of the three body problems that will be developed here is the modified three body Centauri system. The real Centauri system is one with two dominating bodies (those used in the two body problem) and one secondary object. The secondary object is far smaller than the two dominating bodies and as such, results in a simple elliptical orbit for that body while the two body problem presented above models the primary bodies well. Since the goal of the three body problems is to stress the integrators, the third body has been inflated in its mass and velocity to provide a more chaotic evolution. The evolution of the three body problem here is not periodic and has no regular orbit. As such, it provides an excellent opportunity to test how the integrators perform when large numbers of sharp direction changes are present in the system. The scaling variables for the modified three body Centauri system are: $m_{ref} = 1.989x10^{30}$, $r_{ref} = 5.326x10^{12}$, $v_{ref} = 3.0x10^{4}$, and $t_{ref} = 1.285x10^{9}$. For this reference system, the initial conditions are given by:

$$X = \begin{bmatrix} -0.5 & 0 & 0 \\ 0.5 & 0 & 0 \\ 0 & 1 & 0 \end{bmatrix}$$

$$V = \begin{bmatrix} 0.01 & 0.01 & 0 \\ -0.05 & 0 & -0.1 \\ 0 & -.01 & 0 \end{bmatrix}$$

$$M = \begin{bmatrix} 1.1 \\ 0.907 \\ 1 \end{bmatrix}$$

3.2.2 Sun-Earth-Moon System

The next three body problem that will be used here is the Sun-Earth-Moon system and will be used in a manner similar to the use of the two body Sun-Earth system in the previous section. The mass differential between the Sun and Moon is two orders of magnitude greater than the difference between the masses of the Sun and Earth. As such, the risk of underflow is very high, and as will be observed, occurs in this system for machine precision of 16 or less. This means a computer with good precision is needed to accurately evolve this system. For a computer without sufficient precision, the reference object that is the Moon is observed as being thrown out of the system because the underflow occurs in the acceleration of the Moon. The scaling variables for this system are: $m_{ref} = 1.989x10^{30}$, $r_{ref} = 1.486x10^{11}$, $v_{ref} = 3.0x10^{4}$, and $t_{ref} = 3.1557x10^{7}$. The initial conditions for this system are:

$$X = \begin{bmatrix} 0 & 0 & 0 \\ 1 & 0 & 0 \\ 1 & 0.002586 & 0 \end{bmatrix}$$

$$V = \begin{bmatrix} 0 & 0 & 0 \\ 0 & 0.99074 & 0 \\ -0.0341 & 0 & 0 \end{bmatrix}$$

$$M = \begin{bmatrix} 1 \\ 0.0000030025 \\ 0.000000036943 \end{bmatrix}$$

3.2.3 Sun-Earth-Jupiter System

The next system that will be evolved is the Sun-Earth-Jupiter system. This system is a fairly simple system presenting with two elliptical orbits around a dominating primary body. This system is an interesting case study, however, because the two elliptical orbits present in the system have different necessary time steps to reach convergence. The time step needed to accurately evolve the lower acceleration orbit (Jupiter in this case) is much longer than the time step needed to accurately evolve the higher acceleration orbit (Earth in this case). This makes the system interesting to study because only 300 steps on the interval are needed to accurately evolve Jupiter's orbit, while the Earth's orbit needs about 1000 steps on the interval to stabilize to an elliptic orbit. The reference variables for this system are: $m_{ref} = 1.989x10^{30}$, $r_{ref} = 7.7858x10^{11}$, $v_{ref} = 3.0x10^{4}$, and $t_{ref} = 3.1557x10^{7}$. With these reference variables, the initial conditions of the system are given by:

$$X = \begin{bmatrix} 0 & 0 & 0 \\ 0.19086 & 0 & 0 \\ 0 & 1 & 0 \end{bmatrix}$$

$$V = \begin{bmatrix} 0 & 0 & 0 \\ 0 & 0.99074 & 0 \\ -0.43566 & 0 & 0 \end{bmatrix}$$

$$M = \begin{bmatrix} 1 \\ 0.0000030025 \\ 0.00095425 \end{bmatrix}$$

3.2.4 Sun-Jupiter-Saturn System

The next system that will be studied is the Sun-Jupiter-Saturn system. This system is very similar to the Sun-Earth-Jupiter system with the notable exception that the masses of the two secondary bodies only differ by one order of magnitude rather than three. This, combined with the longer distance from the Sun, means that both will have lower accelerations than the Earth as described in the previous problem. These lower accelerations mean a longer time step is acceptable to evolve this system. That makes this system relevant in terms of future research. Adaptive algorithms are commonplace in numerical integration today. The difference here in step size needed to evolve the low acceleration orbits of the Sun-Jupiter-Saturn system and the higher acceleration of the Earth in the Sun-Earth-Jupiter system is significant to developing a future adaptive algorithm for symplectic integration. Changing step size according to the varied accelerations is a good approach for developing an adaptive algorithm. The reference variables for this system are: $m_{ref} = 1.989x10^{30}$, $r_{ref} = 7.7858x10^{11}$, $v_{ref} = 3.0x10^{4}$, and $t_{ref} = 3.1557x10^{7}$. With these scaling variables, the initial conditions are:

$$X = \begin{bmatrix} 0 & 0 & 0 \\ 0 & 1 & 0 \\ -1.9299 & 0 & 0 \end{bmatrix}$$

$$V = \begin{bmatrix} 0 & 0 & 0 \\ -0.43566 & 0 & 0 \\ 0 & -0.32242 & 0 \end{bmatrix}$$

$$M = \begin{bmatrix} 1 \\ 0.00095425 \\ 0.00028572 \end{bmatrix}$$

3.2.5 Sun-Venus-Mercury System

The next system that will be examined here is the Sun-Venus-Mercury system. The Sun-Venus-Mercury system fills a role similar to the role of the Sun-Earth-Moon system, but the two primary bodies are within one order of magnitude of each other which will help to find the limits of the integrators in terms of underflow on the accelerations. In this system, the expected behavior is two elliptical orbits for Venus and Mercury. However, underflow will again cause the smallest body to be thrown out of the system. The way it is thrown out differs from the Sun-Earth-Moon system. In the Sun-Earth-Moon system, the Moon was thrown out immediately because its mass was too small to get any acceleration. In the Sun-Venus-Mercury system, Mercury is thrown out at a slower rate. This is because its mass differential from the Sun is not as large as the difference between the Moon and the Sun. The behavior that is observed due to the overflow is a spiral outward rather than a constant velocity path out of the system. The scaling variables for this system are: $m_{ref} = 1.989x10^{30}$, $r_{ref} = 6.4936x10^{10}$, $v_{ref} = 3.0x10^{4}$, and $t_{ref} = 3.1557x10^{6}$. With these reference variables, the initial conditions in reference units are:

$$X = \begin{bmatrix} 0 & 0 & 0 \\ -1 & 0 & 0 \\ 1.6555 & 0 & 0 \end{bmatrix}$$

$$V = \begin{bmatrix} 0 & 0 & 0 \\ 0 & -1.667 & 0 \\ 0 & 1.674 & 0 \end{bmatrix}$$

$$M = \begin{bmatrix} 1 \\ 0.0000003285 \\ 0.0000024470 \end{bmatrix}$$

3.2.6 Randomly Generated Three Body System

The final system that will be examined here is the randomly generated three body system. This randomly generated system is developed using the same motivation as the randomly generated two body systems. Here three masses are chosen to be relatively similar. Then random initial positions and velocities are chosen to exhibit some unique and interesting behavior. In this system, the positions and velocities are chosen to display an oscillatory behavior in all three bodies. The sharp oscillations in the system offer extreme stress to the symplectic integrators in the same fashion as the modified three body Centauri system. It will be observed in the results, that the convergence to the true solution requires a very small time step for the integrators. Even at the maximum time step used throughout this research, the integrators struggle to converge for this system. The scaling variables for this system are: $m_{ref} = 1.989x10^{30}$, $r_{ref} = 1.486x10^{11}$, $v_{ref} = 3.0x10^{4}$, and $t_{ref} = 3.1557x10^{7}$. With these scaling variables, the initial conditions for the randomly generated three body system are:

$$X = \begin{bmatrix} 0 & 0 & 0 \\ 0 & 1 & 0 \\ 0 & 0 & -1 \end{bmatrix}$$

$$V = \begin{bmatrix} 0 & -0.6132 & 0 \\ 0 & 0 & 0.9156 \\ -1.12 & 0 & 0 \end{bmatrix}$$

$$M = \begin{bmatrix} 1 \\ 0.9 \\ 0.8 \end{bmatrix}$$

The expected behaviors of the three body systems are summarized in the following table.

Table 2: This table gives the expected behavior for each three body system.

System	Expected Behavior
3 Body Centauri	Completely Chaotic
Sun-Earth-Moon	Small Elliptical Orbit and Regular Elliptical Orbit
Sun-Earth-Jupiter	Two Regular Elliptical Orbits
Sun-Jupiter-Saturn	Two Regular Elliptical Orbits
Sun-Venus-Mercury	One Rapid Elliptical Orbit and One Regular Elliptical Orbit
Random 3	Oscillating Patterns

4 RESULTS

In the previous sections, a number of symplectic integration techniques and sample systems were developed to run N-body simulations. In this section, the results of the evolutions will be presented. The first section will cover the Python implementation of the BDF method for developing reference systems. Then the code for implementing symplectic integrators for the two and three body systems will be developed and a method will be described for calculating error between the reference and symplectic trajectories. After the code is introduced, the specific evolutions for varying time steps over a fixed time interval using all four symplectic integrators will be presented. After the evolutions are presented, the error calculations will be given. Once the fixed interval evolutions are completed, a short study of a select system with a select integrator will be conducted on a long-time interval. This long-time evolution is done with the purpose of showing the strength of symplectic integrators in long-time galactic evolutions when compared to tradition BDF methods for the same problem.

4.1 Implementation

The first step in presenting the results of this research is to present the computer implementation of the BDF methods and symplectic integrators. This will be done by detailing the exact process and functionality of the programs written to accomplish the evolutions using BDF methods and symplectic integrators. After the BDF implementation is discussed, the reference systems will be given for all of the two and three body sample systems. After the implementation of symplectic integrators is discussed, the symplectic evolutions will be presented for each two and three body system using fifty, three hundred, five hundred, one thousand, and five thousand steps for each of the four symplectic integrators.

4.1.1 BDF Methods

The first step in presenting the results of this research is to present the computer implementation of all the methods being used beginning with the BDF methods used to generate the reference systems. As discussed previously, for short-time simulations like the majority of those used in this research, BDF methods are sufficient to evolve these systems with decent accuracy. Rather than writing code to handle implementation of the BDF methods, this research will make use of the scipy.integrate.odeint method included in the scipy package for Python. From the documentation of the method, this method in Python makes use of the 6th order BDF method discussed previously. To use this method, an array holding the relevant differential equations, an array holding the initial conditions, an array holding the time steps, and the relevant constant values are all passed to the method. It then performs the BDF calculations discussed in a previous section to evolve a stiff system of ordinary differential equations. There is only one relevant method to write to allow this program to work and that is a method to calculate and return the relevant derivatives defining the equations of motion for the system. This is done by directly calculating the scaled differential equations that were discussed previously. The returned value from this function is the array that is passed to the scipy.integrate.odeint method as the system of differential equations to be solved. Now the reference systems for each two and three body problem generated using the sixth order BDF method are given by:

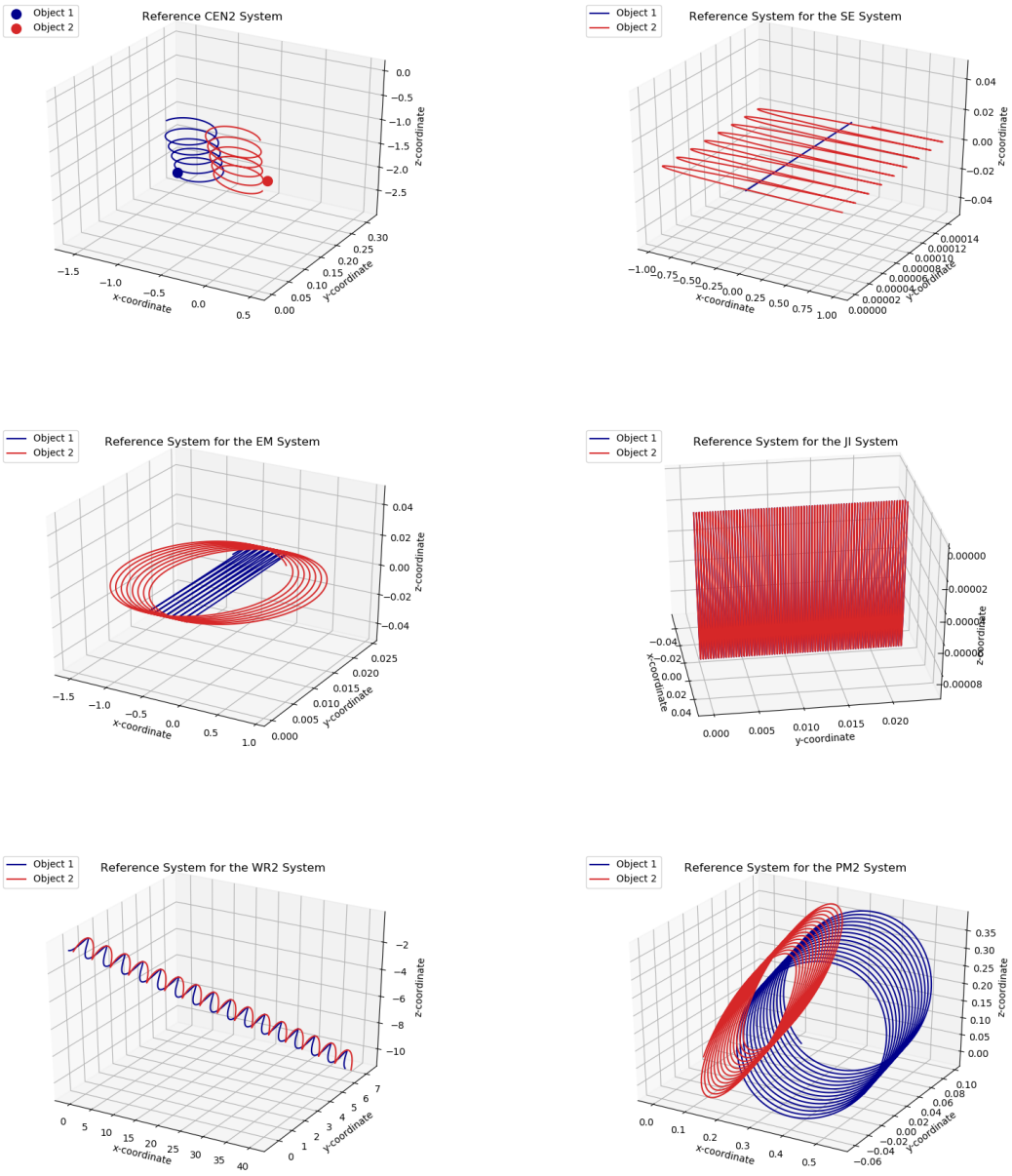

Figure 3: These are the two body reference systems generated using the 6th order BDF method. In order starting in the top left, they are: 2 Body Centauri, Sun-Earth, Earth-Moon, Jupiter-Io, Random 1, and Random 2.

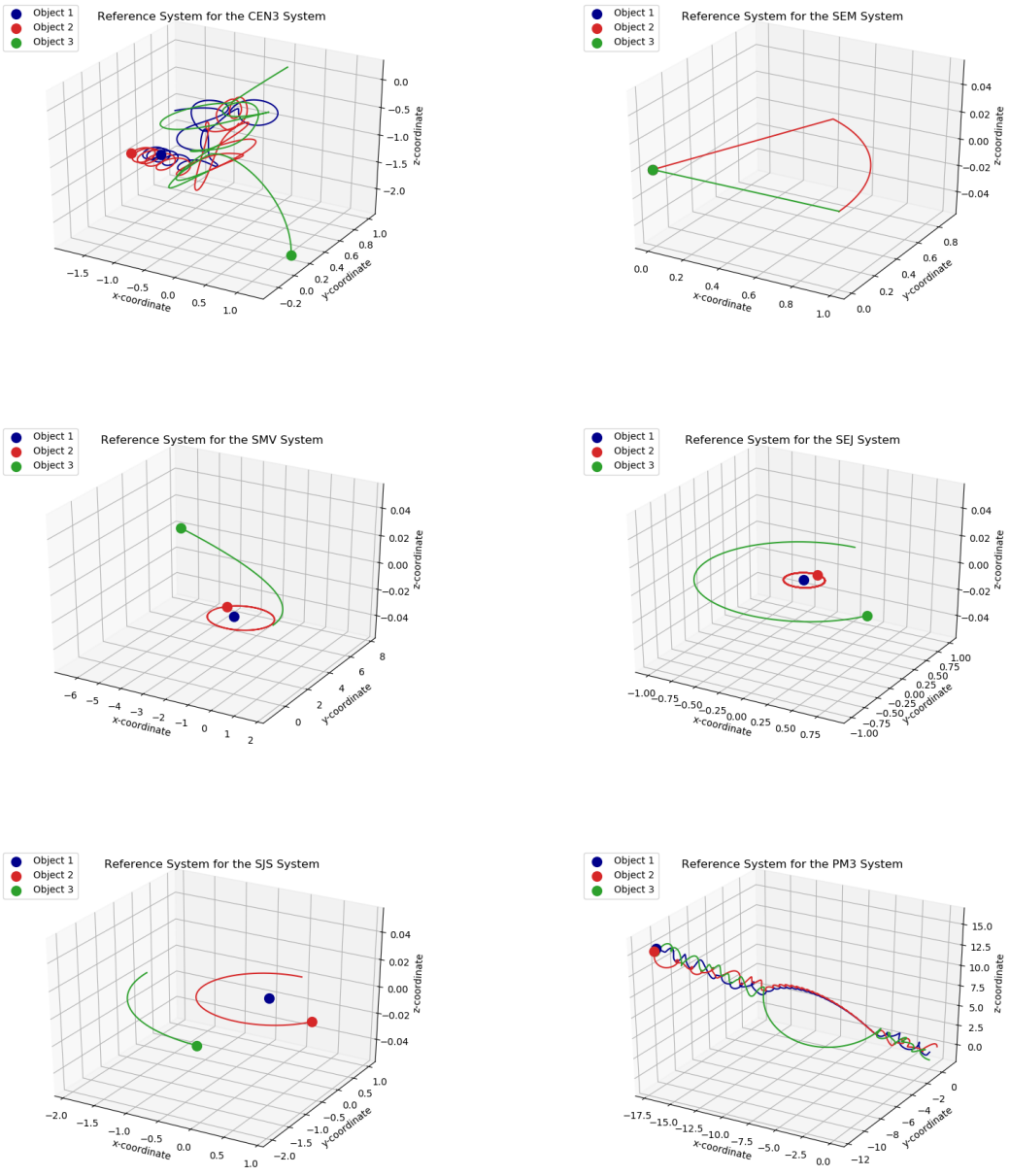

Figure 4: These are the three body reference systems generated using the 6th order BDF method. In order starting in the top left, they are: 3 Body Centauri, Sun-Earth-Moon, Sun-Mercury-Venus, Sun-Earth-Jupiter, Sun-Jupiter-Saturn, and Random.

These images give the reference evolution of each of the two and three body sample systems. The reader should note the wide variety of system types. Many of the two body systems share elliptical orbits, but have different mass conditions as discussed previously.

Many of the three body systems display drastically different behaviors. Each of these systems represents a unique challenge for the symplectic integration techniques. It should also be noted that several of the systems (Sun-Earth-Moon, Sun-Venus-Mercury, and Jupiter-Io) have reference systems which differ significantly from the other systems being used. These systems will be covered in more detail in the section covering error calculations. For the remainder of these systems, their symplectic evolutions and their errors from these reference systems will be discussed in the next two sections.

4.1.2 General Symplectic Integration

The next step in presenting the results of this research is to present the implementation of the symplectic integrators. As no Python packages have general implementation for symplectic integration, the task is more difficult. The code will require the use of two unique methods. The first method that needs to be written is the step function that will perform the evolution for each time step. This is done by passing the initial positions, velocities, masses, time step size, a coefficient matrix defined in the section on symplectic integrators and an acceleration function to the method. The step method then creates a list of coefficients that will be iterated over in parallel. Then for each coefficient, it updates the velocities using an acceleration function derived from the particle particle method discussed in [34] and then updates the positions using the updated velocities. The second method to implement is a method to do the integration over every time step. To do this, a method is given the initial positions, velocities, masses, an acceleration function, a coefficient matrix, and an array holding every time step to calculate the approximation at. The method simply uses the stepping function at every time step and stores the values before returning the final trajectory. For purposes of this research, the methods used are not written to make use of an arbitrary N-body system. A program with the modification to accept a general position and velocity matrix for any N-body system was written but was found to perform significantly

slower than the methods using individual vectors for each initial condition of each body. Now the symplectic evolutions for each of the two and three body systems are presented using each of the four integrators with fifty steps, three hundred steps, five hundred steps, one thousand steps, and five thousand steps. The images are grouped by step size with each of the four integrators being presented with the same step size simultaneously.

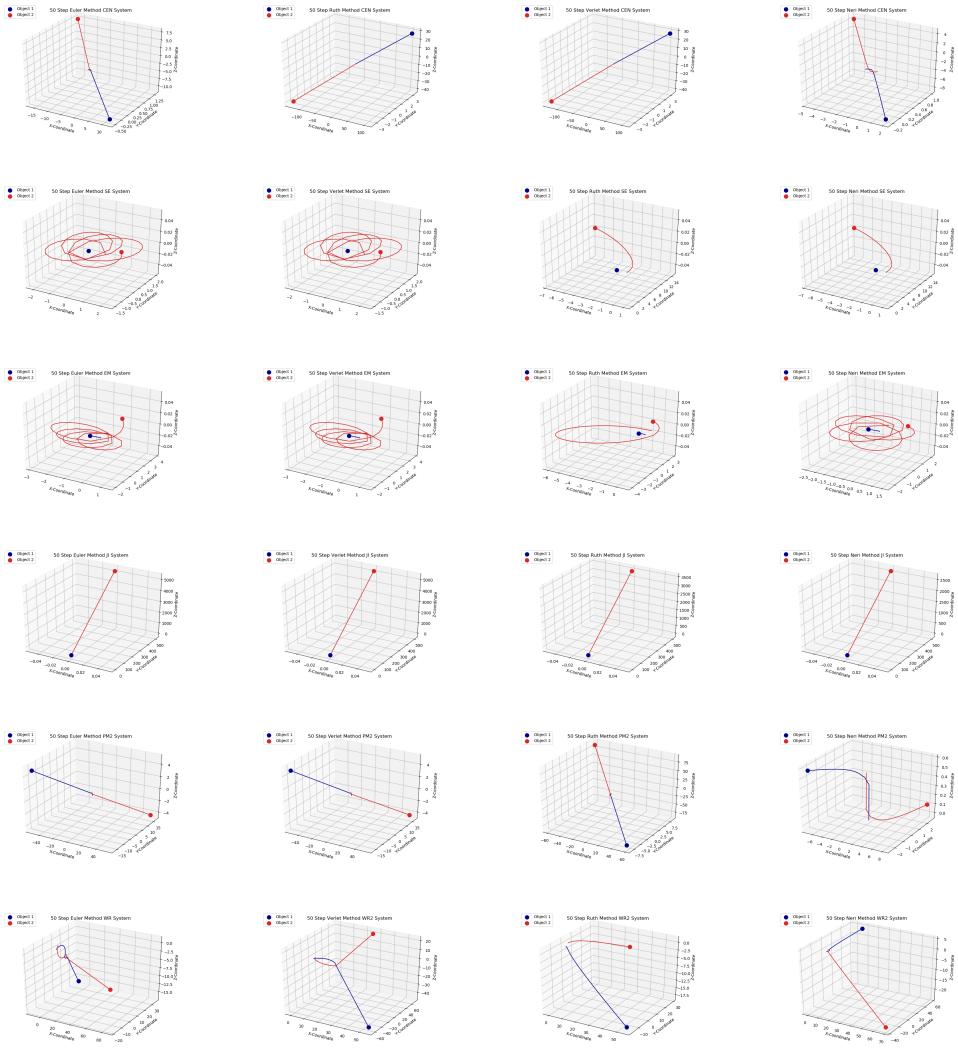

Figure 5: These are the 50 step symplectic integrations for the 2 body systems. They are in groups of four from top to bottom with each row giving a different system. From left to right in each row, the images give the Euler, Verlet, Ruth, and Neri methods applied to the system. From top to bottom, the systems are the 2 Body Centauri, Sun-Earth, Earth-Moon, Jupiter-Io, Random 1, and Random 2.

From these images, it is clear that fifty steps along the eight unit time reference interval is not sufficient to accurately evolve the two body systems. The two body Centauri system, the Jupiter-Io system, and both randomly generated systems explode immediately. They do not attempt to follow the orbits that were discussed when the systems were introduced. The Sun-Earth and Earth-Moon systems attempt to rotate, but do not follow the regular elliptical orbits that are expected. The lack of convergence to the solution for any of the sample systems here will be discussed more when the error profiles for these integrations are given. The important note for this step size is that a shorter step size is needed to approach convergence.

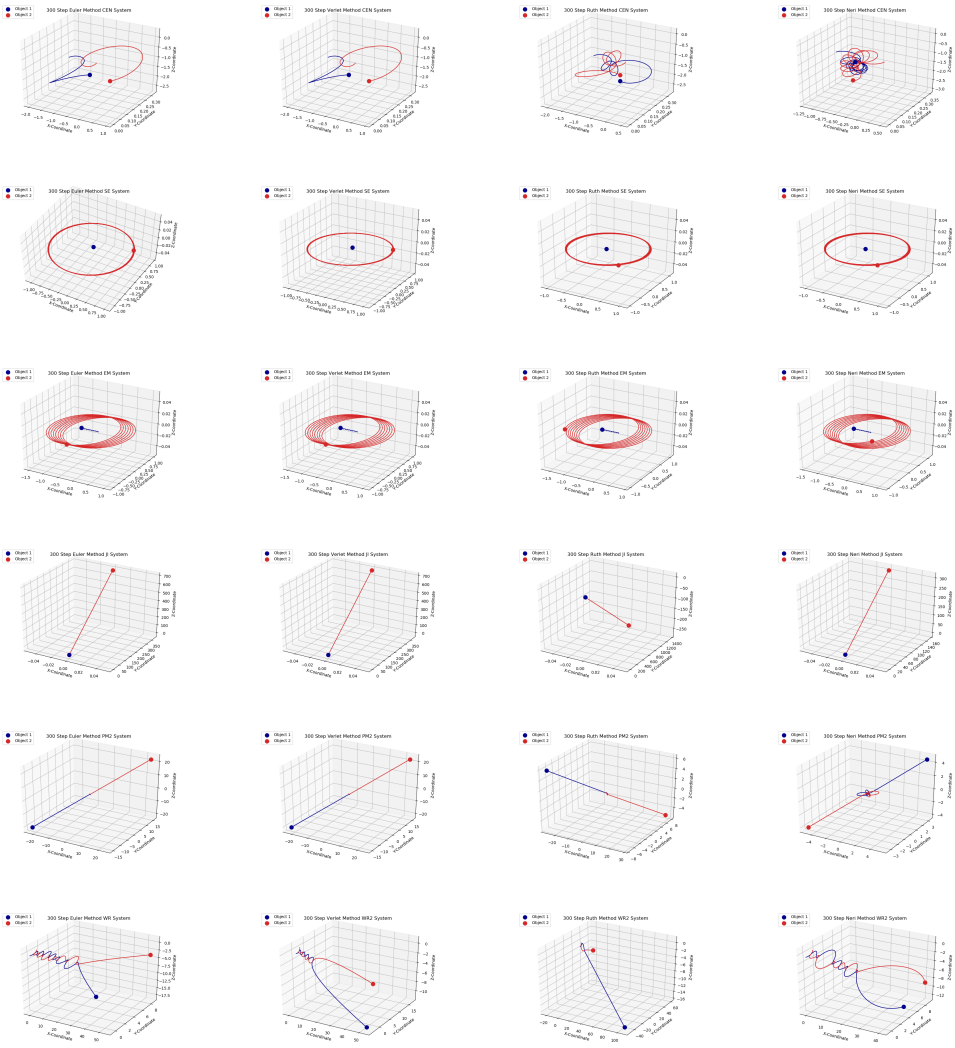

Figure 6: These are the 300 step symplectic integrations for the 2 body systems. They are in groups of four from top to bottom with each row giving a different system. From left to right in each row, the images give the Euler, Verlet, Ruth, and Neri methods applied to the system. From top to bottom, the systems are the 2 Body Centauri, Sun-Earth, Earth-Moon, Jupiter-Io, Random 1, and Random 2.

From these images, it becomes clear that systems experiencing extremely stable orbits are beginning to converge to stable elliptical orbits. The Sun-Earth and Earth-Moon systems are already approaching stable elliptical orbits. However, the other four systems are still exploding or orbiting in wild patterns. This means that for a general N-body problem, a step size of $\Delta t = .02667$ is not sufficient to accurately evolve the systems. However, as

was discussed earlier, adaptive algorithms are commonplace today in numerical integration. This means that for a general N-body problem, an adaptive algorithm could be coded to use a step size this short for stable elliptical orbits like those displayed in the Sun-Earth and Earth-Moon system.

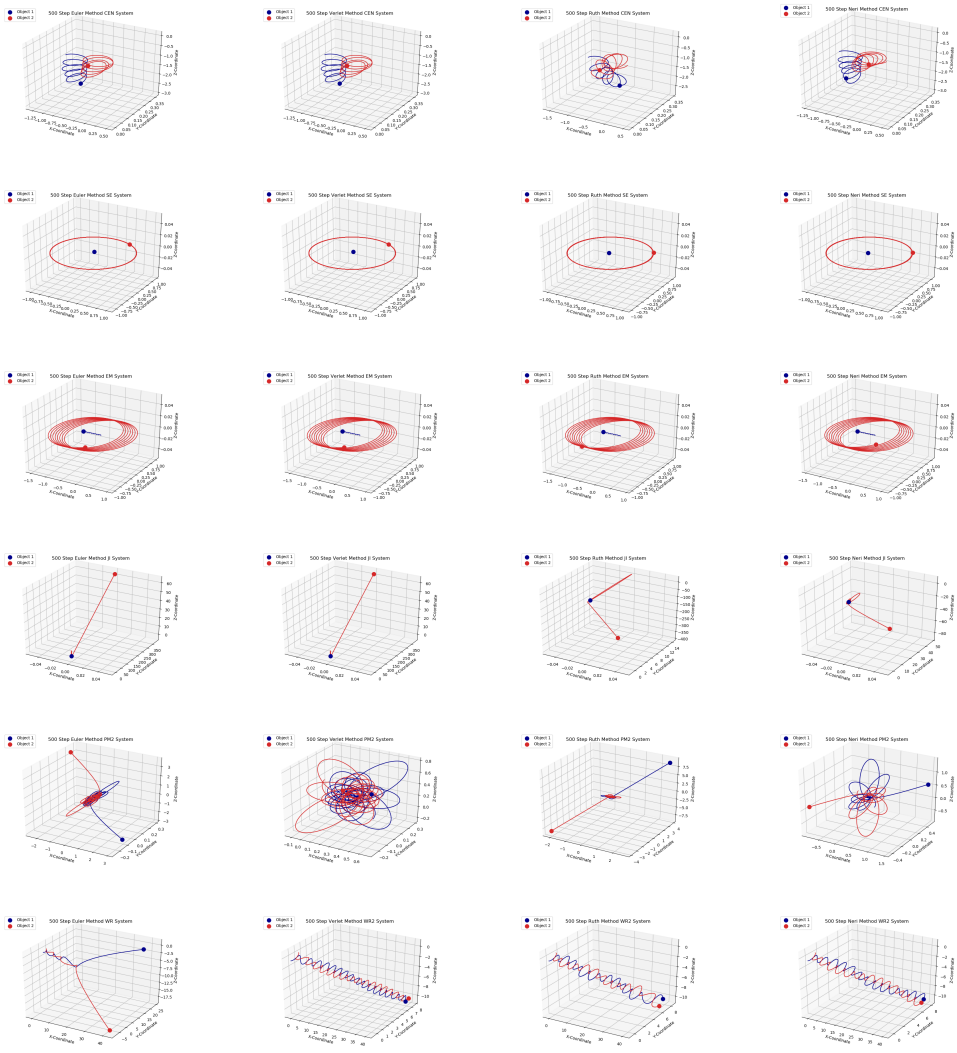

Figure 7: These are the 500 step symplectic integrations for the 2 body systems. They are in groups of four from top to bottom with each row giving a different system. From left to right in each row, the images give the Euler, Verlet, Ruth, and Neri methods applied to the system. From top to bottom, the systems are the 2 Body Centauri, Sun-Earth, Earth-Moon, Jupiter-Io, Random 1, and Random 2.

From these images, it is clear that stable evolutions of the Sun-Earth and Earth-Moon

systems have been reached for the symplectic integrators. The difference in evolution shape is minimal between the three hundred step integrations and the five hundred step integrations, but as is evident in the error graphs presented in the next section, the symplectic integrators are continuing to improve as the step size decreases for the systems which are already stable for longer time steps. For the symplectic schemes that are not the symplectic Euler method, the second randomly generated system is also beginning to converge. The two body Centauri system and the first randomly generated system are also beginning to display structure in the system. This indicates that the step size is approaching a value that will allow the systems to converge to the reference systems. However, the Jupiter-Io system is continuing to explode suggesting that this step size is not sufficient for arbitrary N-body systems. This can give additional guidance for future development of a general adaptive algorithm for arbitrary N-body systems and symplectic scheme.

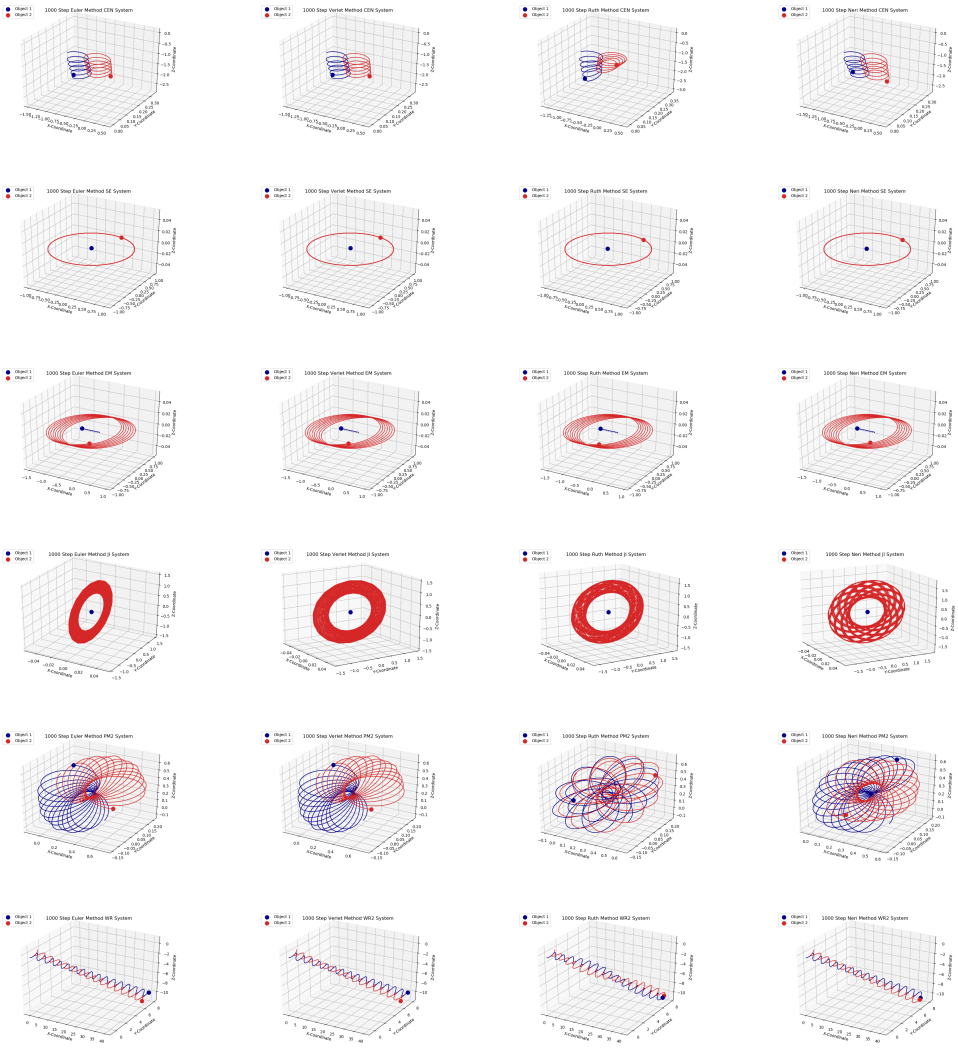

Figure 8: These are the 1000 step symplectic integrations for the 2 body systems. They are in groups of four from top to bottom with each row giving a different system. From left to right in each row, the images give the Euler, Verlet, Ruth, and Neri methods applied to the system. From top to bottom, the systems are the 2 Body Centauri, Sun-Earth, Earth-Moon, Jupiter-Io, Random 1, and Random 2.

In these evolutions, the stability of the Sun-Earth and Earth-Moon systems are again verified which offers additional evidence that a suitable step size has been reached for these systems. Additionally, the two body Centauri system and the second randomly generated system are both beginning to converge. The Jupiter-Io system still displays instability in its orbit but has begun to display elliptical motion which is a strong improvement from

the previous step sizes. The first randomly generated system is also displaying a much clearer structure, but does not display the expected behavior from the reference system. This means that this step size is enough to approximate many of these two body systems, but it is not going to be sufficient to approximate an arbitrary N-body problem.

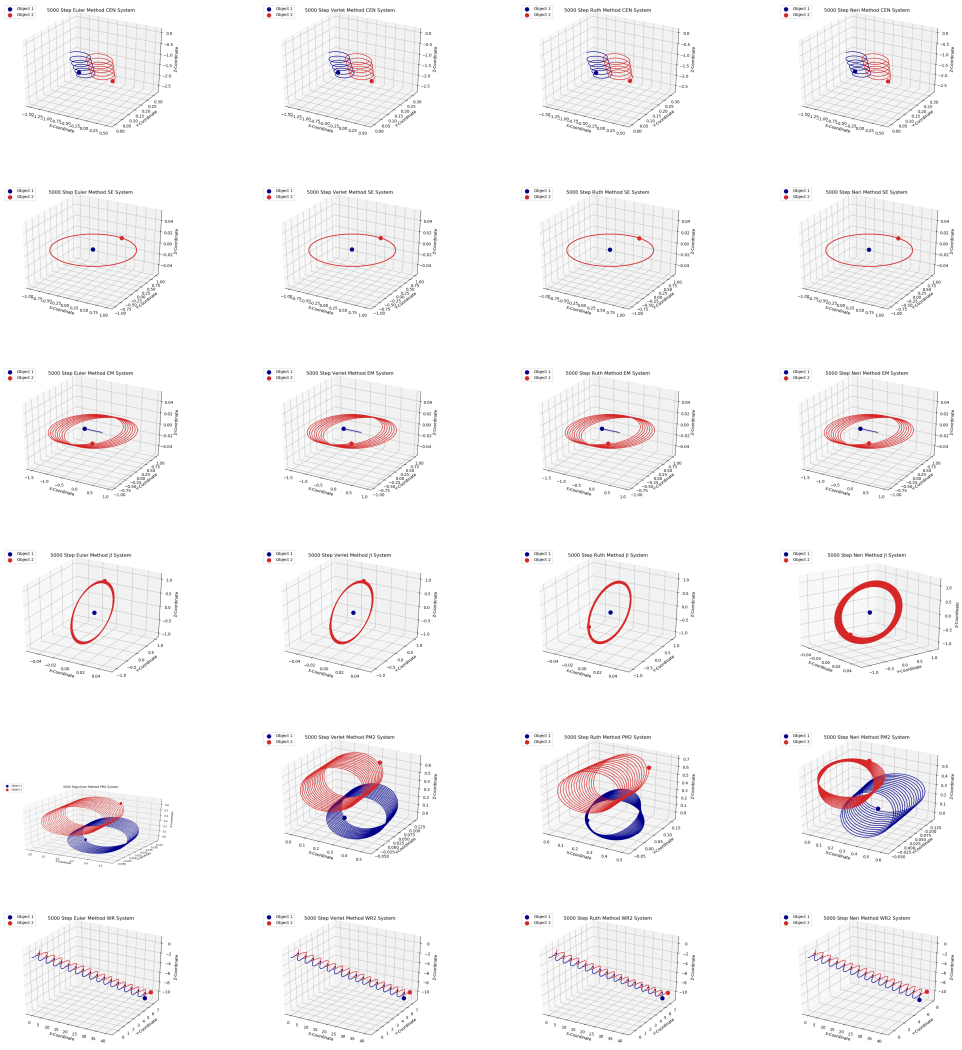

Figure 9: These are the 5000 step symplectic integrations for the 2 body systems. They are in groups of four from top to bottom with each row giving a different system. From left to right in each row, the images give the Euler, Verlet, Ruth, and Neri methods applied to the system. From top to bottom, the systems are the 2 Body Centauri, Sun-Earth, Earth-Moon, Jupiter-Io, Random 1, and Random 2.

From these images, all six two body systems have begun to converge to the reference systems generated by the BDF method. This indicates that for these two body problems and for systems with similar orbital structures, a step size of $\Delta t = .0016$ is sufficient to approach accurate evolutions. However, the rapid rotations in the first randomly generated system are still causing issues suggesting that very high accelerations require much shorter time steps to converge to the true orbits of the system. The convergence for the other five systems, however, offer evidence for the development of an adaptive algorithm that this time step is sufficient to accurately track orbits for the stable, low-acceleration trajectories that are common in gravitational systems.

The convergent step for each integrator on each of the two body problems is summarized in the following table.

Table 3: This table summarizes the orders of accuracy and convergent step sizes for each integration method on each system.

System	Integrator	Accuracy	Steps Needed
2 Body Centauri	Euler	$O(\Delta t)$	1000
	Verlet	$O(\Delta t^2)$	1000
	Ruth	$O(\Delta t^3)$	5000
	Neri	$O(\Delta t^4)$	1000
Sun-Earth	Euler	$O(\Delta t)$	300
	Verlet	$O(\Delta t^2)$	300
	Ruth	$O(\Delta t^3)$	300
	Neri	$O(\Delta t^4)$	300
Earth-Moon	Euler	$O(\Delta t)$	300
	Verlet	$O(\Delta t^2)$	300
	Ruth	$O(\Delta t^3)$	300
	Neri	$O(\Delta t^4)$	300
Jupiter-Io	Euler	$O(\Delta t)$	5000
	Verlet	$O(\Delta t^2)$	5000
	Ruth	$O(\Delta t^3)$	5000
	Neri	$O(\Delta t^4)$	5000
Random 1	Euler	$O(\Delta t)$	5000
	Verlet	$O(\Delta t^2)$	5000
	Ruth	$O(\Delta t^3)$	5000
	Neri	$O(\Delta t^4)$	5000
Random 2	Euler	$O(\Delta t)$	1000
	Verlet	$O(\Delta t^2)$	500
	Ruth	$O(\Delta t^3)$	500
	Neri	$O(\Delta t^4)$	500

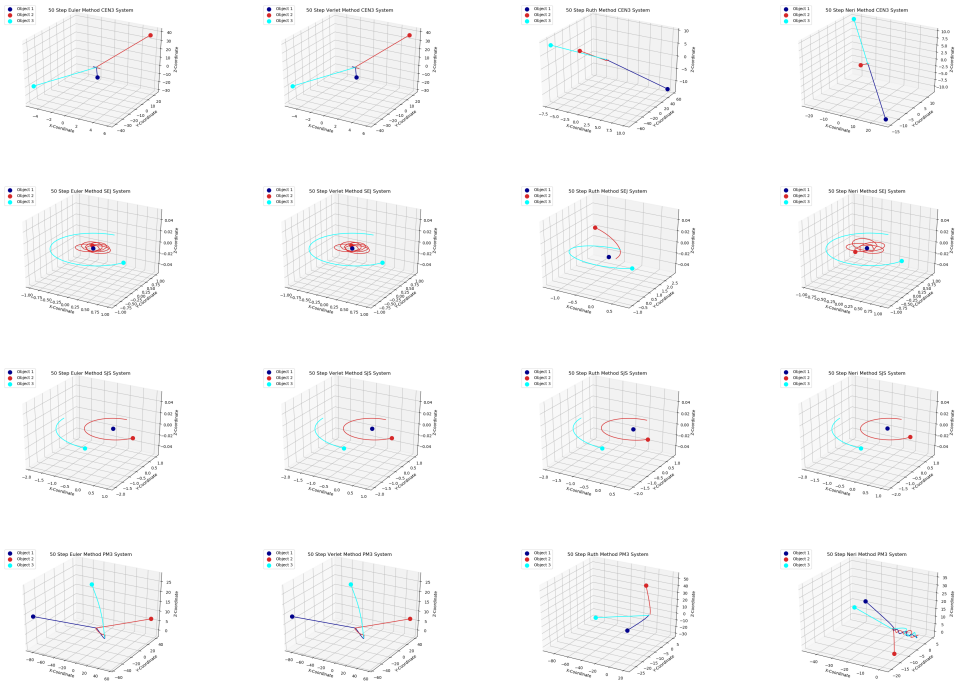

Figure 10: These are the 50 step symplectic integrations for the 3 body systems. They are in groups of four from top to bottom with each row giving a different system. From left to right in each row, the images give the Euler, Verlet, Ruth, and Neri methods applied to the system. From top to bottom, the systems are the 3 Body Centauri, Sun-Earth-Jupiter, Sun-Jupiter-Saturn, and Random.

In the fifty step evolutions for the three body problems, similar behavior is observed for two of the four systems analyzed in this section as was observed for the two body problems. The three body Centauri system and the randomly generated three body system both explode for this long of a time step suggesting that it is not sufficient to accurately track the trajectories for these random motions. However, the Sun-Jupiter-Saturn system is already convergent to the reference system for this time step. This is because Jupiter and Saturn are very far away from the primary body in the system and as a result have very low accelerations. Additionally, in the Sun-Earth-Jupiter system, Jupiter is still convergent for this time step. This offers additional evidence that low acceleration objects in an N-body system are able to be accurately tracked by longer time steps which continues to build evidence of using calculated acceleration as a means to build an adaptive algorithm

for general symplectic integration. It also offers evidence that instability in the orbit of one secondary body caused by an insufficient time step will not cause the orbit of another secondary object to suffer significantly.

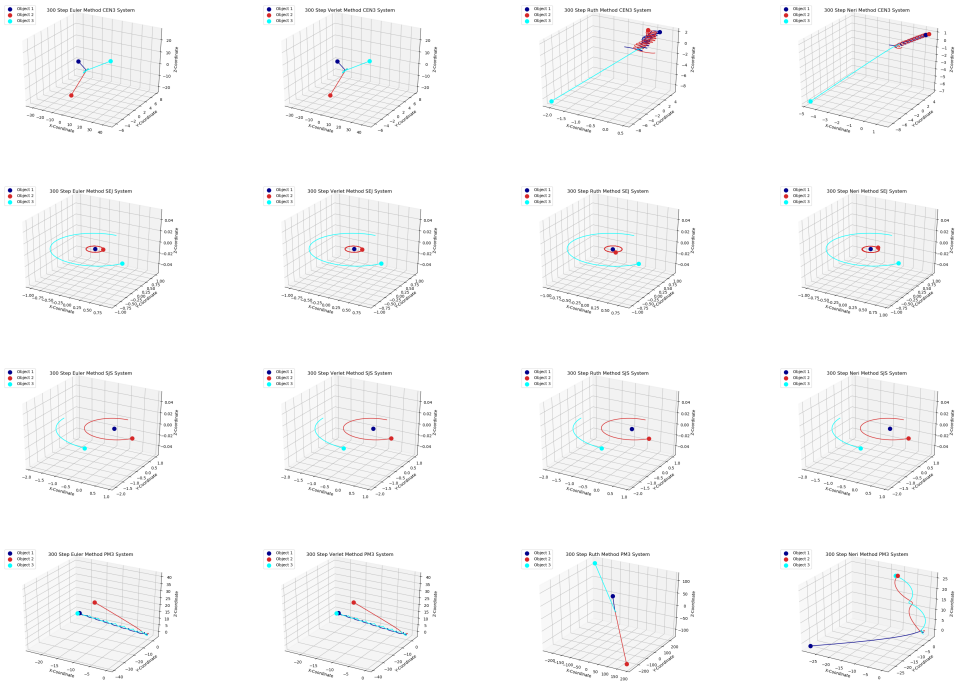

Figure 11: These are the 300 step symplectic integrations for the 3 body systems. They are in groups of four from top to bottom with each row giving a different system. From left to right in each row, the images give the Euler, Verlet, Ruth, and Neri methods applied to the system. From top to bottom, the systems are the 3 Body Centauri, Sun-Earth-Jupiter, Sun-Jupiter-Saturn, and Random.

In these systems, the convergence to the reference system seen in the fifty step integrations holds for the Sun-Jupiter-Saturn system giving firm evidence that the step sizes used were sufficient to accurately evolve these systems. The Earth in the Sun-Earth-Jupiter system is now also displaying a stable elliptical orbit as expected, which suggests that moderate acceleration elliptical orbits can be tracked by a step size of $\Delta t = .02667$. Notably, the trajectory of the Earth begins to converge for the same step size as in the Sun-Earth two body problem. However, the two highly chaotic systems of the three body Centauri system and the randomly generated three body system continue to display divergent behavior.

This suggests that this step size is not sufficient to evolve arbitrary N-body problems. It is important to note, however, that at this time step both of the more chaotic systems are beginning to display some structure which suggests the integrators are insufficient at this time step rather than unable to evolve the systems entirely.

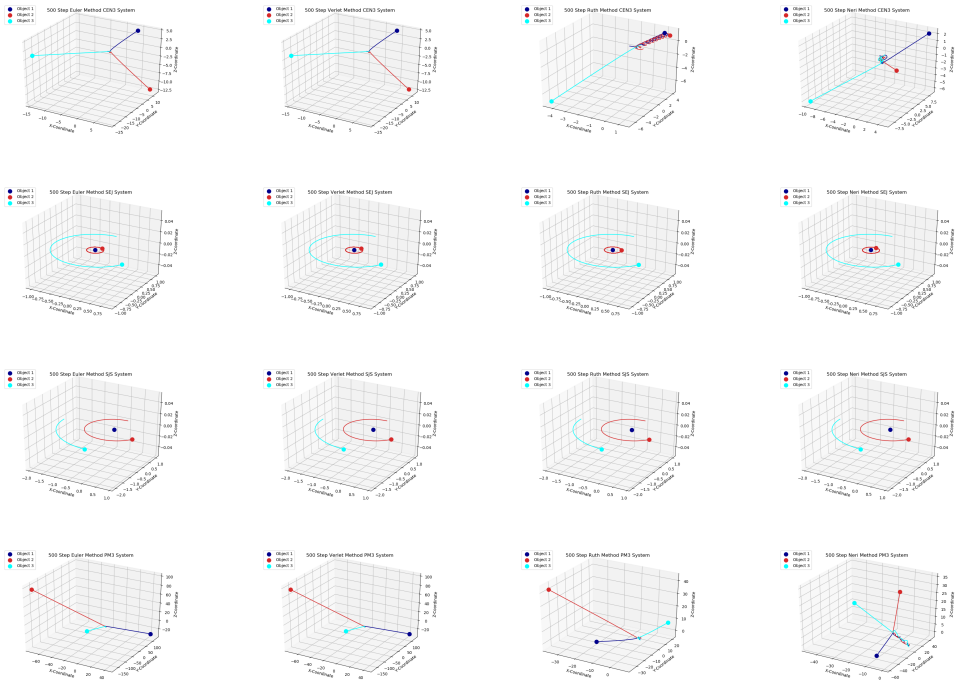

Figure 12: These are the 500 step symplectic integrations for the 3 body systems. They are in groups of four from top to bottom with each row giving a different system. From left to right in each row, the images give the Euler, Verlet, Ruth, and Neri methods applied to the system. From top to bottom, the systems are the 3 Body Centauri, Sun-Earth-Jupiter, Sun-Jupiter-Saturn, and Random.

For these five hundred step integrations and the two remaining step sizes, the Sun-Earth-Jupiter and Sun-Jupiter-Saturn systems remain stable with slightly improving error as will be discussed in the next section of this paper. However, the three body Centauri system and the randomly generated three body system are still exploding. This means that this step size is still insufficient to evolve highly chaotic N-body problems. It is important to note, however, that in the randomly generated system, the objects are beginning to converge. The divergence occurs once the system begins to narrow before flaring as in the reference

system. This point corresponds to a high acceleration point in the system. This suggests that the divergence at this time step is related to the issue of high accelerations which has been observed throughout this section.

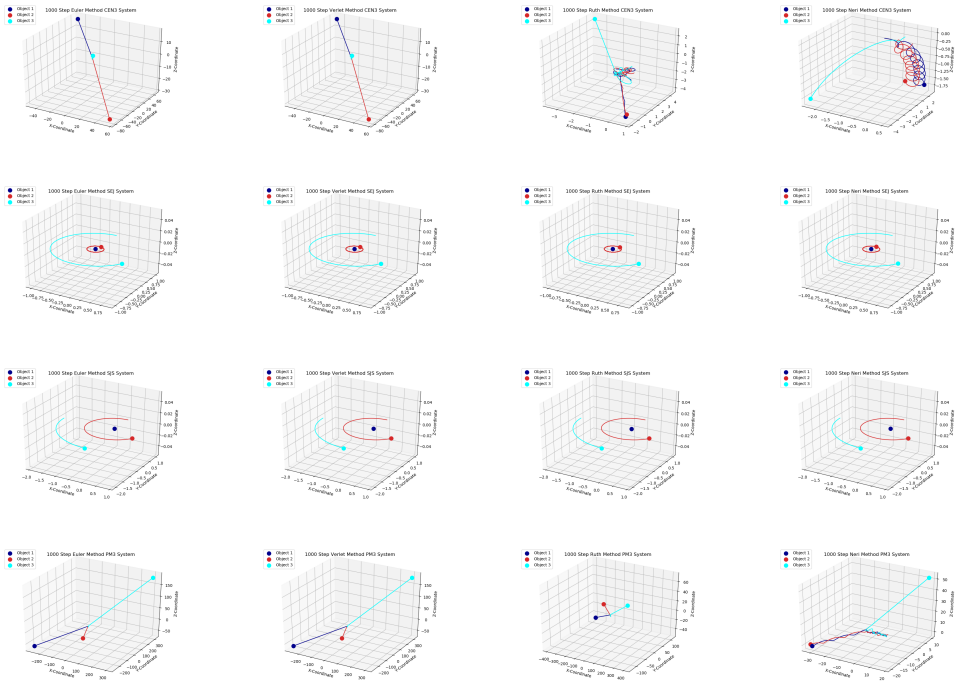

Figure 13: These are the 1000 step symplectic integrations for the 3 body systems. They are in groups of four from top to bottom with each row giving a different system. From left to right in each row, the images give the Euler, Verlet, Ruth, and Neri methods applied to the system. From top to bottom, the systems are the 3 Body Centauri, Sun-Earth-Jupiter, Sun-Jupiter-Saturn, and Random.

For the time step of $\Delta t = .008$, the two stable systems continue to have low error. The three body Centauri system and the randomly generated three body system also continue to display structure for some integrators. The important note for these integrations is the significant difference between the low order integrators and the high order integrators. For example, at this time step, the Euler method is still highly divergent and explodes rapidly. However, the Neri method displays strong indications of converging to the reference system for this time step. This is evidence of why higher order methods are preferred to low order methods when evolving arbitrary N-body systems even when they suffer at long step sizes.

As discussed in the results of the two body systems, the low order integrators can converge for longer time steps in stable systems. However, the high order methods are far better at handling arbitrary problems. Given that galactic systems are described by billions of bodies over hundreds of millions of years, this ability to predict chaotic behavior with a smaller time step is more important than being able to predict stable behavior with a smaller time step.

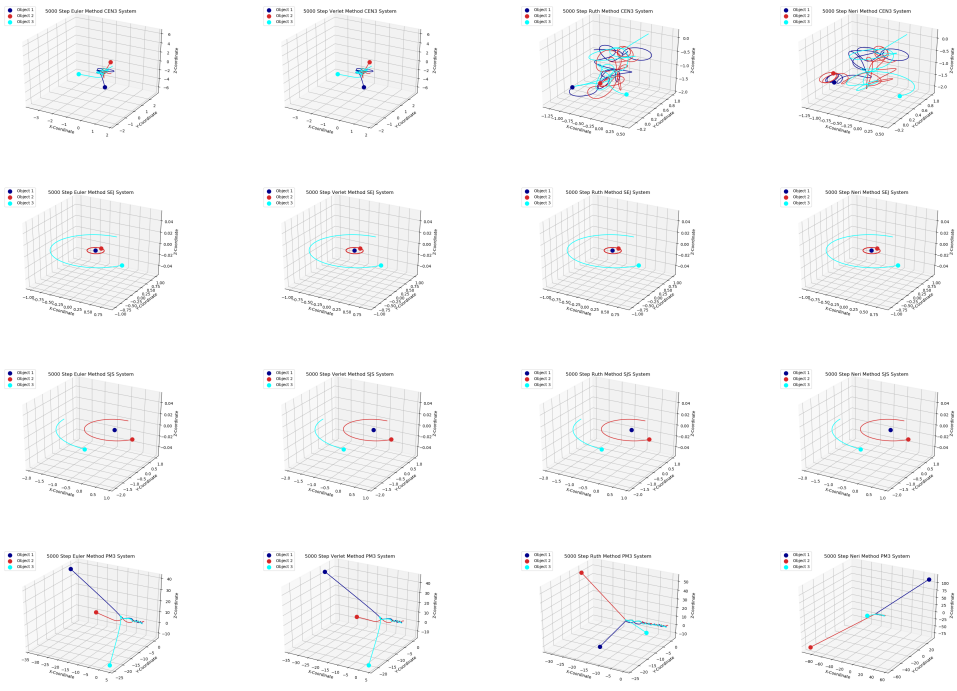

Figure 14: These are the 5000 step symplectic integrations for the 3 body systems. They are in groups of four from top to bottom with each row giving a different system. From left to right in each row, the images give the Euler, Verlet, Ruth, and Neri methods applied to the system. From top to bottom, the systems are the 3 Body Centauri, Sun-Earth-Jupiter, Sun-Jupiter-Saturn, and Random.

In the final integrations on the three body systems, the idea that higher order integrators are needed to evolve chaotic systems is reinforced. In the three body Centauri system, the Ruth and Neri methods are starting to track the motion that is observed in the reference system. This suggests that the two high order integrators are beginning to converge to the reference system in this case. However, in the very high acceleration orbits present in the

randomly generated three body system, none of the integrators are accurately tracking the orbits of all three bodies past the point where the system reaches its highest accelerations. This, again, reinforces the idea that high accelerations cause the symplectic integrators to struggle. However, with a much shorter time step, the symplectic integrations do converge to the reference system. In trials, they were found to approach convergence at least for a time step of $\Delta t = .000016$. This means that additional work is needed to ensure stability in arbitrary N-body problems.

A summary of the convergent step count for each integrator on each three body system is given in the following table.

Table 4: This table summarizes the orders of accuracy and rates of convergence for integrator on each of the 3 body systems given.

System	Integrator	Accuracy	Steps Needed
3 Body Centauri	Euler	$O(\Delta t)$	5000
	Verlet	$O(\Delta t^2)$	5000
	Ruth	$O(\Delta t^3)$	5000
	Neri	$O(\Delta t^4)$	5000
Sun-Earth-Moon	Euler	$O(\Delta t)$	Underflow
	Verlet	$O(\Delta t^2)$	Underflow
	Ruth	$O(\Delta t^3)$	Underflow
	Neri	$O(\Delta t^4)$	Underflow
Sun-Earth-Jupiter	Euler	$O(\Delta t)$	50/300
	Verlet	$O(\Delta t^2)$	50/300
	Ruth	$O(\Delta t^3)$	50/300
	Neri	$O(\Delta t^4)$	50/300
Sun-Jupiter-Saturn	Euler	$O(\Delta t)$	50
	Verlet	$O(\Delta t^2)$	50
	Ruth	$O(\Delta t^3)$	50
	Neri	$O(\Delta t^4)$	50
Sun-Venus-Mercury	Euler	$O(\Delta t)$	Underflow
	Verlet	$O(\Delta t^2)$	Underflow
	Ruth	$O(\Delta t^3)$	Underflow
	Neri	$O(\Delta t^4)$	Underflow
Random 3	Euler	$O(\Delta t)$	Does Not Converge
	Verlet	$O(\Delta t^2)$	Does Not Converge
	Ruth	$O(\Delta t^3)$	Does Not Converge
	Neri	$O(\Delta t^4)$	Does Not Converge

4.2 Error Calculations

The third step in presenting results of this research is to give the implementation for the two types of error calculations used. Fortunately, for vectors and matrices, Python has the numpy.linalg.norm method in the numpy library. This method accepts a general matrix or vector and an order argument. In then returns a norm corresponding to the order argument given. To find the largest error between the symplectic evolution and the reference evolution of each system, the infinity norm is used on the vector of point wise errors at each time step. The point wise errors are calculated using the 2-norm of the difference of the position vectors of the symplectic and reference trajectories at the same point in time. The infinity norm then returns the largest of these values. To find the distance from the reference trajectory to the symplectic trajectory, the 2-norm of the point wise error vector is taken. This gives the overall distance of the entire symplectic path to the reference path. Here the errors are given for each symplectic integrator with each of the given step sizes over the short-time interval grouped in the same way as the results of the symplectic integrations.

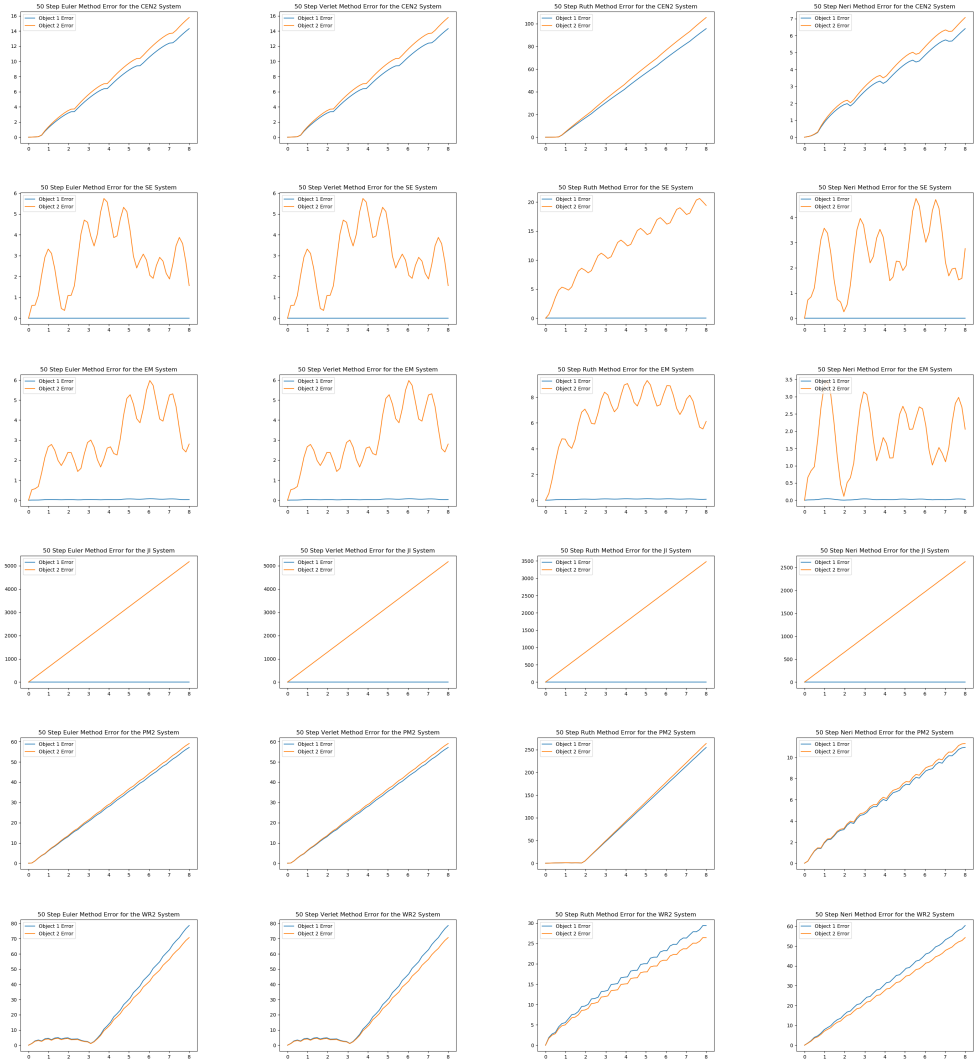

Figure 15: These are the errors for the 50 step symplectic integrations for the 2 body systems taken with respect to the reference systems. They are in groups of four from top to bottom with each row giving a different system. From left to right in each row, the images give the Euler, Verlet, Ruth, and Neri methods applied to the system. From top to bottom, the systems are the 2 Body Centauri, Sun-Earth, Earth-Moon, Jupiter-Io, Random 1, and Random 2.

As was discussed briefly in the previous section, short time steps are needed to drive symplectic integrators to convergence. In the previous section, it was observed that the 50 step integrations were unable to adequately evolve any of the two body systems. Most of the systems immediately exploded with the bodies moving directly away from each other.

The systems that did not exhibit that behavior experienced chaotic motion in the secondary body of the system. These behaviors are reflected in the error calculations for the fifty step integrations on the two body systems. For the Sun-Earth and the Earth-Moon systems, the secondary body oscillates in error suggesting the symplectic integrator is not resulting in system collapse, but is not accurately predicting the evolution either. In the other four systems, the error explodes rapidly suggesting that the bodies of the system are flying away from the reference orbits constantly. This is exactly the behavior that was observed in the previous section when the evolutions were given.

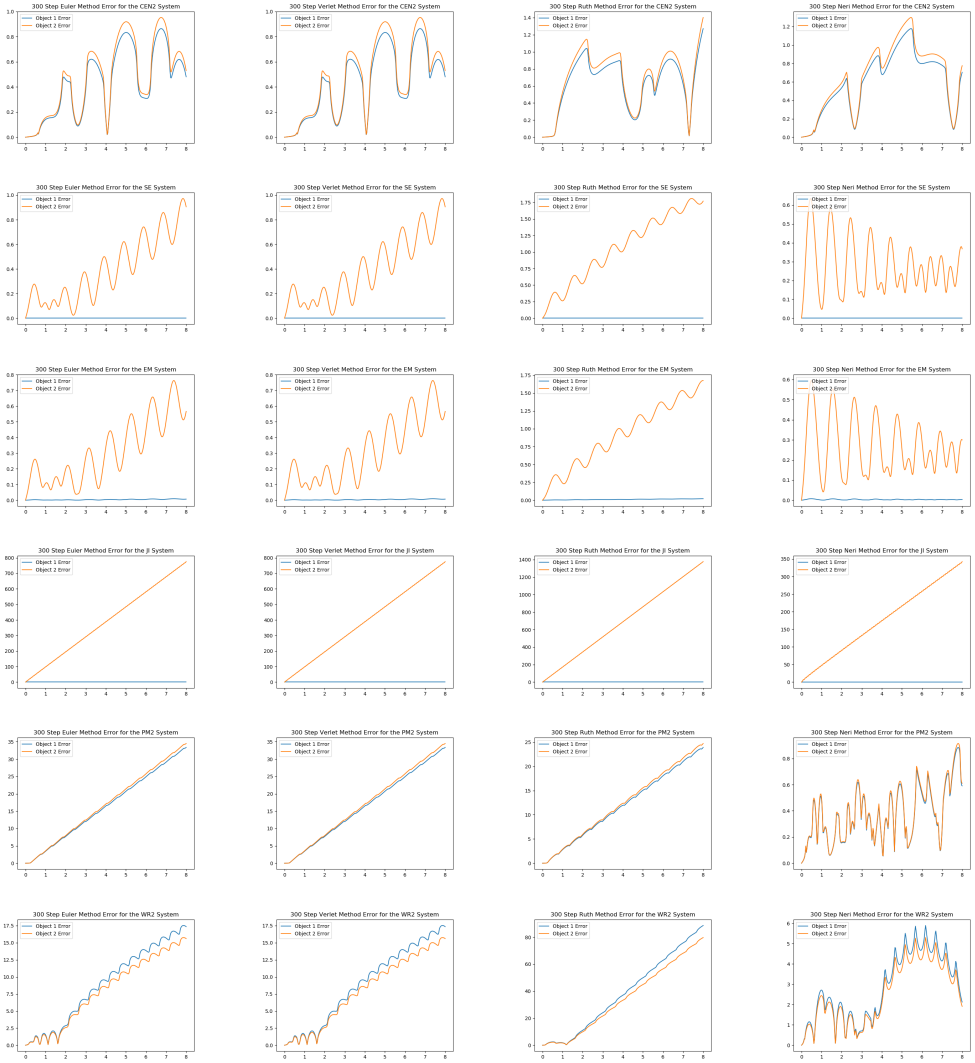

Figure 16: These are the errors for the 300 step symplectic integrations for the 2 body systems taken with respect to the reference systems. They are in groups of four from top to bottom with each row giving a different system. From left to right in each row, the images give the Euler, Verlet, Ruth, and Neri methods applied to the system. From top to bottom, the systems are the 2 Body Centauri, Sun-Earth, Earth-Moon, Jupiter-Io, Random 1, and Random 2.

In the previous section, the most important note that was made about the three hundred step integrations was that low acceleration orbits such as the ones in the Sun-Earth and Earth-Moon system had already begun to converge. That observation is confirmed in these error graphs. For the systems which had begun to display convergent behavior, the errors

are not climbing linearly as they do in the systems with high acceleration. They do rise over time, but that is due to the steadily increasing error of the BDF method as is discussed elsewhere in this paper. An important note is that the errors oscillate according to where the body is in its orbit, but the symplectic integrators are accurately evolving the most stable orbits for this step size.

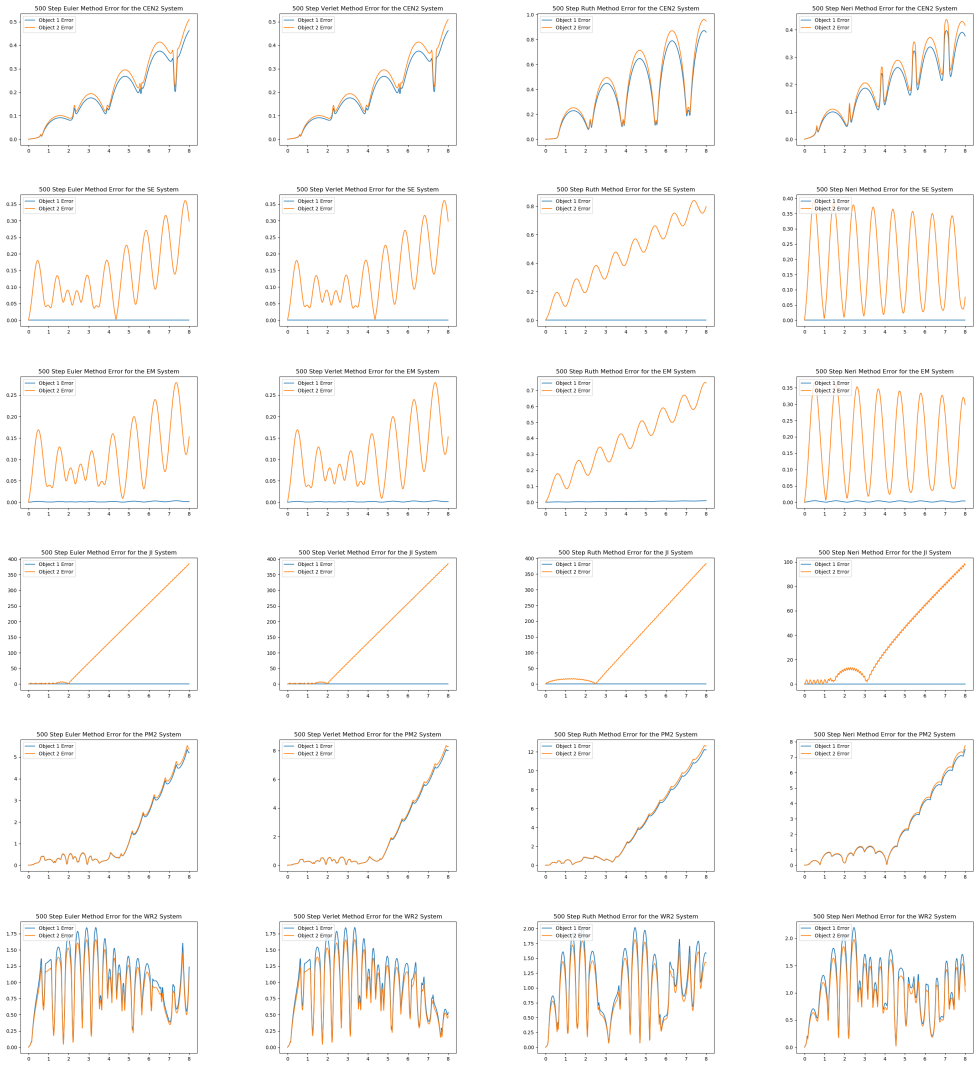

Figure 17: These are the errors for the 500 step symplectic integrations for the 2 body systems taken with respect to the reference systems. They are in groups of four from top to bottom with each row giving a different system. From left to right in each row, the images give the Euler, Verlet, Ruth, and Neri methods applied to the system. From top to bottom, the systems are the 2 Body Centauri, Sun-Earth, Earth-Moon, Jupiter-Io, Random 1, and Random 2.

In the previous section, the orbits developed by the symplectic integration schemes for the two body systems appears consistent as the time step is reduced for the systems that become convergent at an early time step. However, the error graphs show that error is still reducing as the time step is shortened. This behavior is expected for numeric integration.

The error graphs give here also still indicate an exploding behavior for the systems with high accelerations like the Jupiter-Io system and the first randomly generated system.

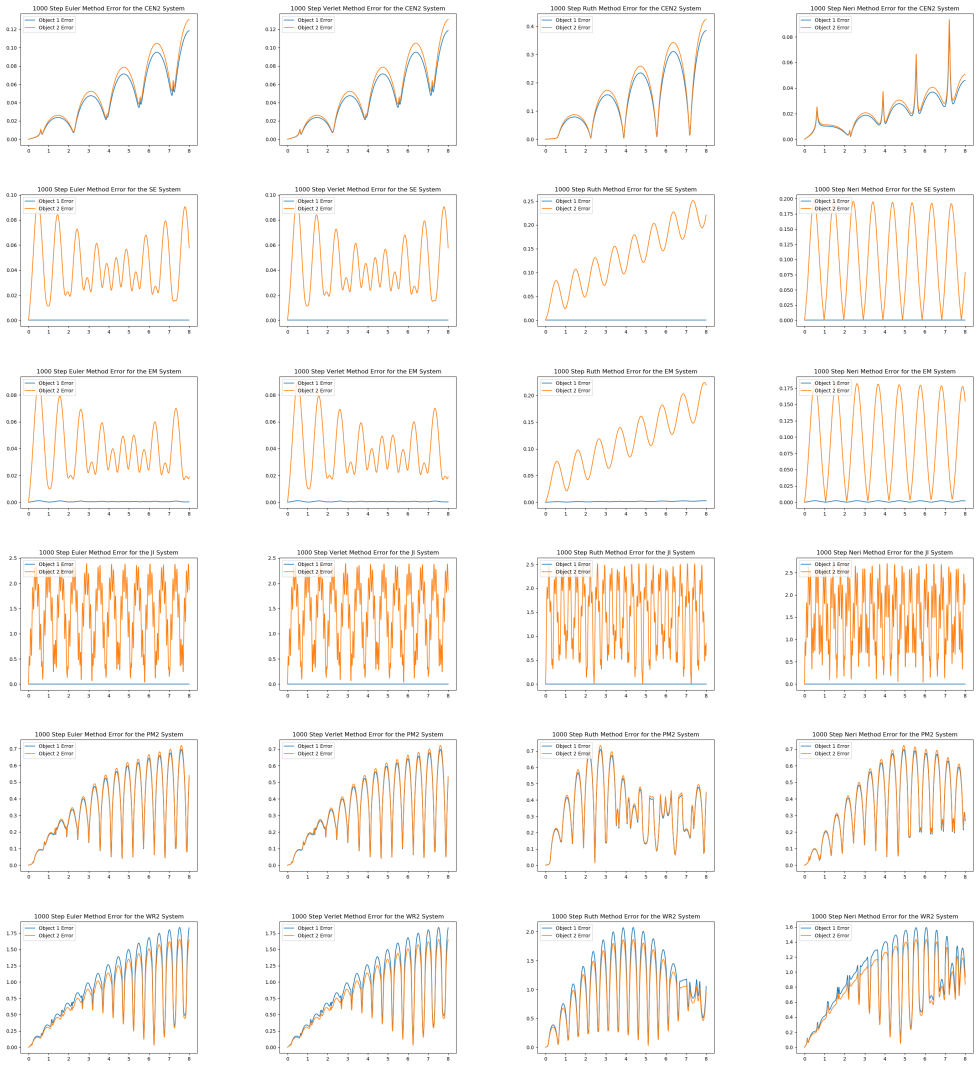

Figure 18: These are the errors for the 1000 step symplectic integrations for the 2 body systems taken with respect to the reference systems. They are in groups of four from top to bottom with each row giving a different system. From left to right in each row, the images give the Euler, Verlet, Ruth, and Neri methods applied to the system. From top to bottom, the systems are the 2 Body Centauri, Sun-Earth, Earth-Moon, Jupiter-Io, Random 1, and Random 2.

For the systems which converge at longer time steps, these error graphs continue to indicate improvement in the integrators. However, at the time step $\Delta t = .008$, the error

graph now indicates stability in the Jupiter-Io system and the first randomly generated two body system as was discussed in the previous section. Rather than climbing linearly as with the shorter time steps, the error graphs oscillate in a fashion similar to the other two body systems. While the oscillations are more chaotic due to the high accelerations, the error graphs clearly indicate that these systems are beginning to converge.

Figure 19: These are the errors for the 5000 step symplectic integrations for the 2 body systems taken with respect to the reference systems. They are in groups of four from top to bottom with each row giving a different system. From left to right in each row, the images give the Euler, Verlet, Ruth, and Neri methods applied to the system. From top to bottom, the systems are the 2 Body Centauri, Sun-Earth, Earth-Moon, Jupiter-Io, Random 1, and Random 2.

For the shortest time step considered in this paper, the error functions are clearly indicating convergence and structure for all six two body problems. The Jupiter-Io system continues to display some instability for the Neri method implementation, but the other three methods all accurately evolve the system. Additionally, the other five systems have

continued to reduce their errors at every time step as the step size has decreased which is expected. The errors for these systems are primarily below a value of 0.05 reference units which indicates strong convergence to the reference system.

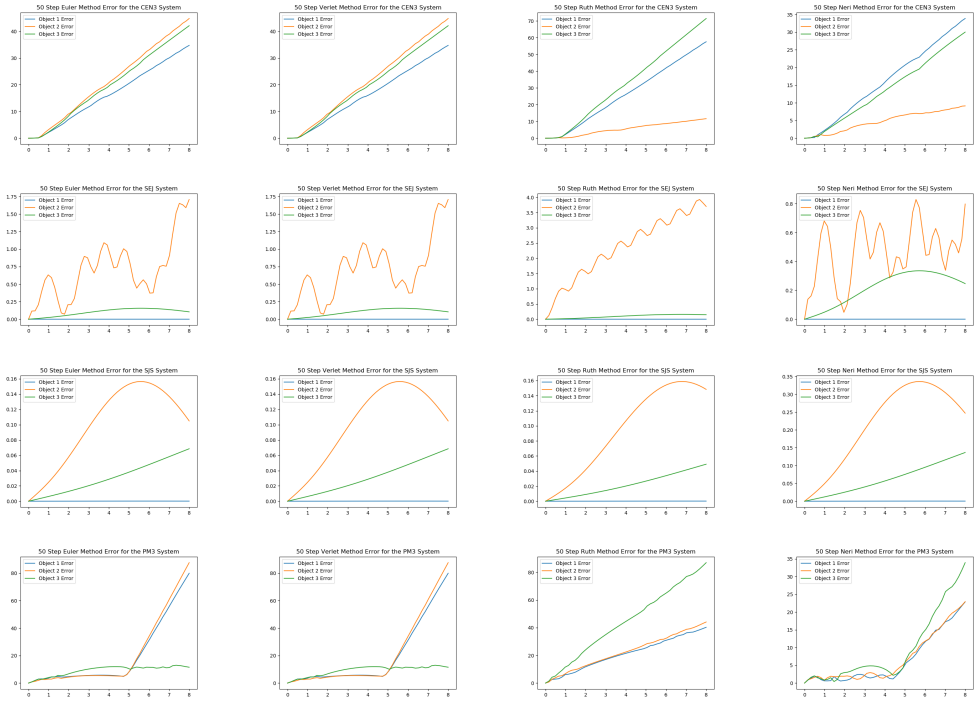

Figure 20: These are the errors for the 50 step symplectic integrations for the 3 body systems taken with respect to the reference systems. They are in groups of four from top to bottom with each row giving a different system. From left to right in each row, the images give the Euler, Verlet, Ruth, and Neri methods applied to the system. From top to bottom, the systems are the 3 Body Centauri, Sun-Earth-Jupiter, Sun-Jupiter-Saturn, and Random.

In the previous section, it was mentioned that long time steps were acceptable to evolve the three body systems with very low accelerations, but the other systems needed much shorter time steps to approach the true trajectories of the bodies in the system. The error graphs presented here clearly support that statement. While the errors are still fairly high for the systems with stable, low acceleration elliptical orbits, the Sun-Earth-Jupiter and the Sun-Jupiter-Saturn system display clear structure in their error graphs already. Additionally, it was mentioned throughout the previous analysis of the integrations that the randomly generated system evolves accurately at the beginning and then diverges as

the accelerations increase. This behavior was difficult to observe from the plots of the trajectories themselves, but it is easily observed here. In the error functions for the randomly generated system, the error remains low before spiking at some point in time. This point in time corresponds to the point when the trajectories of all three bodies pass very near each other before flaring outward in the reference system. These error graphs then also support that high accelerations cause the symplectic integrators to fail as was previously discussed.

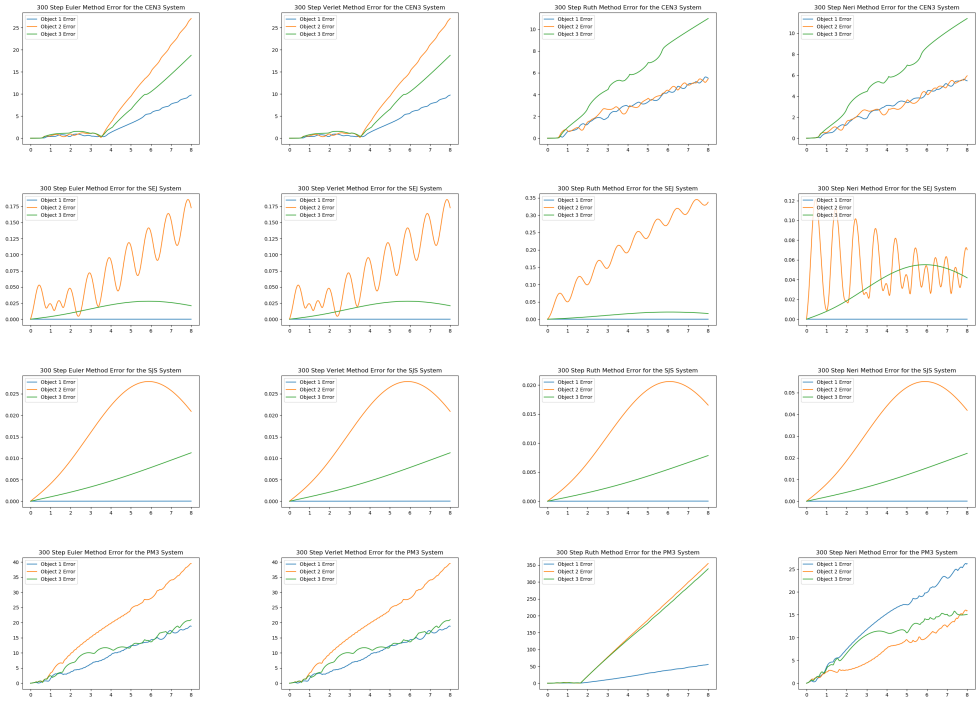

Figure 21: These are the errors for the 300 step symplectic integrations for the 3 body systems taken with respect to the reference systems. They are in groups of four from top to bottom with each row giving a different system. From left to right in each row, the images give the Euler, Verlet, Ruth, and Neri methods applied to the system. From top to bottom, the systems are the 3 Body Centauri, Sun-Earth-Jupiter, Sun-Jupiter-Saturn, and Random.

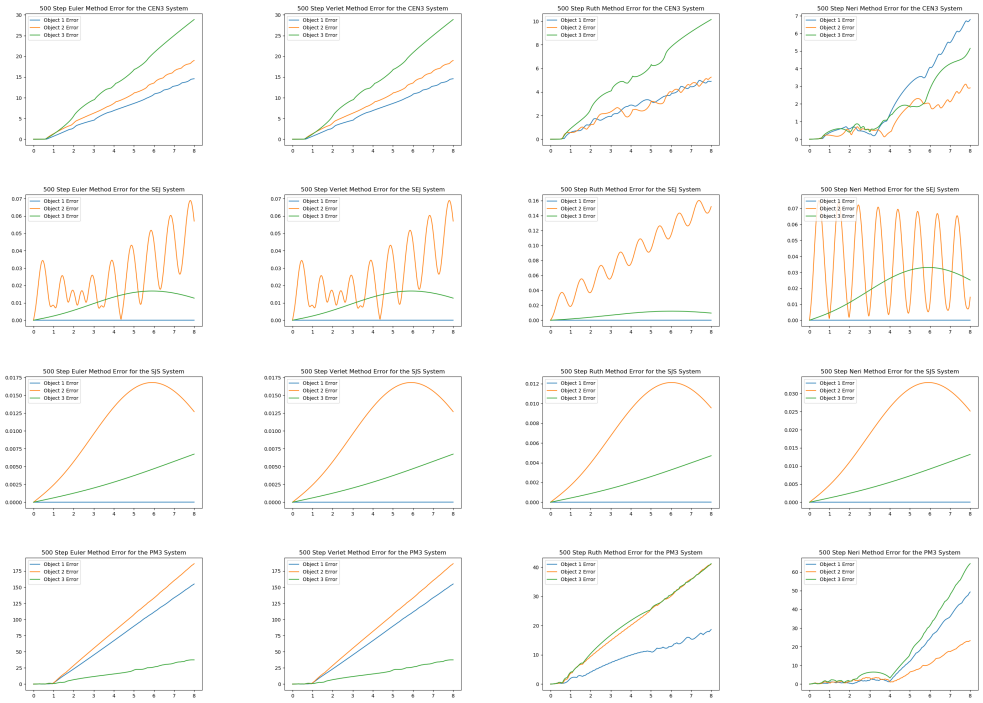

Figure 22: These are the errors for the 500 step symplectic integrations for the 3 body systems taken with respect to the reference systems. They are in groups of four from top to bottom with each row giving a different system. From left to right in each row, the images give the Euler, Verlet, Ruth, and Neri methods applied to the system. From top to bottom, the systems are the 3 Body Centauri, Sun-Earth-Jupiter, Sun-Jupiter-Saturn, and Random.

In the previous section, it was noted that the three hundred and five hundred step integrations were nearly identical for the systems which approach convergence with the longest time step. The error functions presented here continue to support that statement. In these images, it is clear that mesh size is reducing the point wise error of the symplectic trajectories from the reference trajectories as the step size is reduced. The noteworthy behavior in the error plots of the three hundred and five hundred step integrations is the start of convergence in even the three body Centauri system. As was discussed in the previous section, these step sizes are insufficient to accurately evolve the three body Centauri system or the randomly generated system; however, it is clear that the three body Centauri system is extending the time over which the integrations remain accurate before decaying. Ultimately, the randomly generated system continues to fail at the same point in time due

to the very high accelerations on all three bodies at that point.

Figure 23: These are the errors for the 1000 step symplectic integrations for the 3 body systems taken with respect to the reference systems. They are in groups of four from top to bottom with each row giving a different system. From left to right in each row, the images give the Euler, Verlet, Ruth, and Neri methods applied to the system. From top to bottom, the systems are the 3 Body Centauri, Sun-Earth-Jupiter, Sun-Jupiter-Saturn, and Random.

Figure 24: These are the errors for the 5000 step symplectic integrations for the 3 body systems taken with respect to the reference systems. They are in groups of four from top to bottom with each row giving a different system. From left to right in each row, the images give the Euler, Verlet, Ruth, and Neri methods applied to the system. From top to bottom, the systems are the 3 Body Centauri, Sun-Earth-Jupiter, Sun-Jupiter-Saturn, and Random.

In the previous section, the trajectory plots indicated that the three body Centauri system was beginning to converge at these time steps, but still did not accurately track the orbits through the highest acceleration points of the system. For the one thousand and five thousand step integrations, the error graphs are now displaying a clear oscillating structure similar to that present in the stable systems. This indicates that the integrations are attempting to converge (particularly the Ruth and Neri method), but are still struggling with high acceleration parts of the system. It is also clear that the symplectic integrators continue to struggle with accurately tracking past high acceleration parts of the orbits in the randomly generated system. Importantly though, the Ruth and Neri methods both progress further with the five thousand step integration than the previous step sizes. This indicates that a shorter step size is accurately advancing the system past high acceleration

parts of trajectories as is expected. This gives strong evidence that an adaptive algorithm for symplectic integration is necessary.

Two systems have so far been omitted from the previous results discussions. The Sun-Earth-Moon system and the Sun-Venus-Mercury system were left out of previous discussions because of a unique feature that is important to highlight in any numerical research. These two systems have the largest mass differential of any systems used in this research. As a result, these systems both experience underflow errors while calculating the accelerations. The processor used to perform this research has 16 digit machine precision. Both of these systems fall slightly outside of that value when accelerations are calculated. As a result, the systems lose the acceleration of the smallest body in the system after a certain number of time steps and that body is thrown from the system.

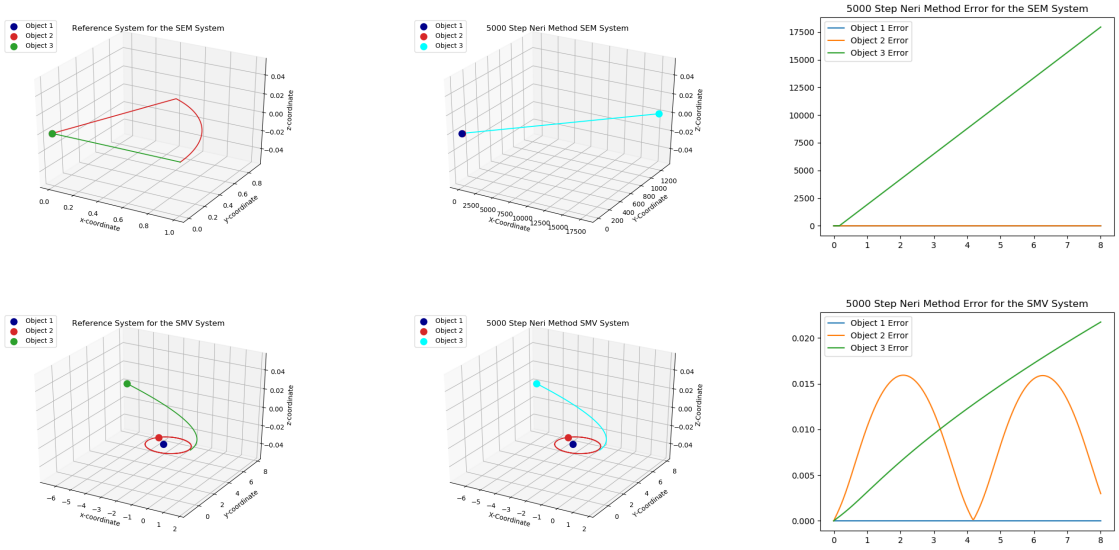

Figure 25: These are the "reference" systems and 5000 step Neri evolutions for the Sun-Earth-Moon and Sun-Venus-Mercury Systems along with the "error" calculaions for these two systems.

In these images it can be seen that the system with the largest mass difference throws its small body out faster than the other. Notably, the moon flies directly out of the system immediately with no acceleration being calculated. Venus in the Sun-Venus-Mercury system, however, is thrown out in a wide spiral. It is clear that the integrator was attempting to properly calculate the accelerations for both of these systems from this example. The underflow error present in these two systems is a reminder to make use of proper technology in addition to proper numerical integration techniques. On a system with more floating point precision than the one used for this research, these systems would evolve normally with elliptical orbits for both secondary bodies in each system.

4.3 Long Time Evolutions

As the final analysis of this research, the four symplectic integration methods will be evolved on a select system. This system will again be evolved using the sixth order BDF methods. However, given the long time evolution of these systems, the expectation for

the BDF method is that it will significantly diverge from the true evolution of the system. To allow an accurate comparison of symplectic method to the BDF method for long time integration, a system with regular and predictable orbits must be used. This section will make use the two body Centauri system. Here the time step will be fixed to $\Delta t = .0016$ which is equivalent to the five thousand step integration on the short time interval used in the previous results. Instead of evolving the system for eight reference time units, the system will be evolved for forty-eight reference time units. In the point wise error plots, the expected behavior is a gradually increasing error between the symplectic evolution and BDF evolution. This increasing error comes from the construction of the BDF method as was shown through the example of the explicit Euler method.

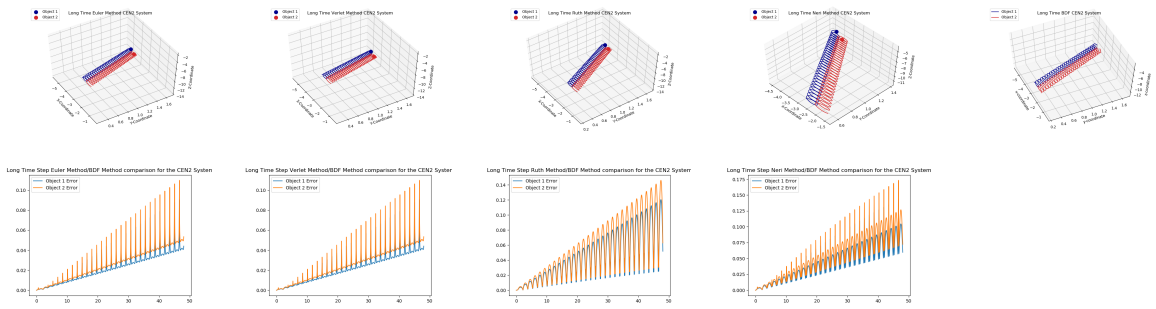

Figure 26: These images give a comparison of long time evolutions of symplectic integrators using a $\Delta t = 0.0016$ reference units time step. These images compare the decay of the BDF method with the same time step as the systems are evolved for longer periods of time. The first row of images gives the CEN2 long time evolutions for each integrator. The second row gives the "error" compared to the BDF evolution.

From these images, it is clear that the error in the positions of both bodies is gradually increasing as the time interval of the evolution is increased. This demonstrates the lack of adequacy of the BDF methods in evolving the N-body problem over very long time intervals. As was discussed earlier, to accurately evolve a galactic system over even a single period of the stars furthest from its center would take an evolution of hundreds of millions of reference time units. The sixth order BDF method is already showing failing accuracy at only forty-eight reference time units with only two bodies. If it had to run for forty-eight

million reference time units on billions of objects, its increasing error would be fatal to any accurate model of an N-body problem. This fatal flaw in the BDF methods is what inspires further research into the numerical integration techniques which can accurately evolve N-body systems over long-time intervals.

5 CONCLUSION

Throughout this paper, the history and construction of the N-body problem has been developed and several numerical integration techniques for evolving systems of ordinary differential equations were explored. By analyzing a variety of time steps for the symplectic integration methods discussed in this paper over a variety of different initial conditions, it was determined that high accelerations cause failure in the approximations of these techniques. It was also found that for low acceleration trajectories such as those present in the Sun-Jupiter-Saturn system, a very long time step is sufficient to accurately track an object. These two facts give strong evidence of the need for developing an adaptive algorithm based on time step accelerations to accurately use general symplectic algorithms to evolve arbitrary N-body systems. Additionally, through an analysis of errors in the trajectories, it was determined that the symplectic methods are able to accurately evolve the trajectories considered in this paper so long as the time step is sufficiently small. A short discussion was also given on the ineffectiveness of using classical BDF methods to numerically integrate arbitrary N-body problems. Even for the two body Centauri system, the BDF method used in this paper diverges significantly for long time intervals. This indicates a need for symplectic algorithms which maintain stability over very long intervals when evolving galactic systems while exploring the N-body problem and dark matter.

REFERENCES

1. Ryden, Barabara and Bradley Peterson. *Foundations of Astrophysics.* Addison-Wesley Publishing Company, 2010.
2. Krane, Kenneth. *Modern Physics.* 3rd ed., John Wiley and Sons, 2012.
3. Zuene, L. *Constraining Supersymmetric Models Using Higgs Physics, Precision Observables, and Direct Searches.* 1st ed., University of Hamburg, 2014.
4. Juillard, A. "Status and Prospects of the EIDELWEISS-III Direct WIMP Search Experiment." *Journal of Low Temperature Physics,* 2016.
5. Barrow-Greene, June. "The Dramatic Episode of Karl Sundman." *Historia Mathematica,* vol. 37, no. 2, 2010, pp. 164-203.
6. Newton, Isaac. *Philosophiae Naturalis Principia Mathematica Vol 1.* 1687.
7. Serway, Raymond and John Jewett. *Physcis for Scientists and Engineeers.* 9th ed., Brooks/Cole Learning, 2014.
8. Chambers, J.E. and G.W. Wetherill. "Making the Terrestrial Planets: N-body Integrations of Planetary Embryos in Three Dimensions." *Icarus,* vol. 136, no. 2, 1998, pp. 304-327.
9. Suvakov, Milovan and V. Dmitrasinovic. "Three Classes of Newtonian Thee-Body Planar Periodic Orbits." *American Physical Society,* vol. 1, no. 1, 1958.
10. Diacu, Florin. "The Solution of the N-body Problem." *The Mathematical Intelligencer,* vol. 18, no. 3, 1996, pp. 66-70.
11. D'Eliseo, Maurizio. "The First-Order Orbital Equation." *American Journal of Physics,* vol. 75, no. 352, 2007.
12. Sundman, Karl. "Memoire sur le probleme des trois corps." *Acta Mathematica,* vol. 36, no. 1, 1913, pp. 105-179.
13. Qiu-Dong, Wang. "The Global Solution of the N-body Problem." *Celestial Mechanics and Dynamical Astronomy,* vol. 50, no. 1, 1990, pp. 73-88.

14. Saari, Donald. "A Visit to the Newtonian N-body Problem via Elementary Complex Variables." *The American Mathematical Monthly,* vol. 97, no. 2, 1990, pp. 105-119.
15. Saari, Donald. "Improbability of Collisions in Newtonian Gravitational Systems." *Transactions of the American Mathematical Society,* vol. 162, 1971, pp. 267-271.
16. Hulkower, Neal. "Central Configurations and Hyperbolic-Elliptic Motion in the Three Body Problem." *Celestial Mechanics,* vol. 21, no. 1, 1980, pp. 37-41.
17. Milnor, John. "On the Concept of Attractor." *Communications in Mathematical Physics,* vol. 99, no. 2, 1985, pp. 177-195.
18. Hunt, Brian; Li, Tien-Yien; Kennedy, Judy and Helena Nusse. *The Theory of Chaotic Attractors.* Springer, 2004.
19. Grebogi, Celso; Ott, Edward and James York. "Chaos, Strange Attractors, and Fractal Basin Boundaries in Nonlinear Dynamics." *Science Washington,* vol. 238, no. 4827, 1987, pp. 632.
20. LaSalle, Joseph and Solomon Lefschetz. *Stability By Lyapunov's Direct Method, with Applications.* New York Academic Press, 1961.
21. Sanz-Sera, J. "Symplectic Integrators for Hamiltonian Problems: An Overview." *Acta Numerica,* vol. 1, 1992, pp. 249-271.
22. Goldstein, Herbert. *Classical Mechanics.* 1922. Addison-Wesley Publishing Company, 2005.
23. Yoshida, Haruo. "Construction of Higher Order Symplectic Integrators." *Physics Letters A,* vol. 150, no. 5, 1990, pp. 262-268.
24. Merritt, David and Eugene Vasiliev. "Orbits Around Black Holes in Triaxial Nuclei." *The Astrophysical Journal,* vol. 726, no. 2, 2011, pp. 61-81.
25. Hairer, Ernst. *Lecture 2: Symplectic Integrators.* TU Munchen Press, 2010.
26. Yoshida, Haruo. "Recent Progress in the Theory and Application of Symplectic Integrators." *Celestial Mechanics and Dynamical Astronomy,* vol. 56, no. 1, 1993, pp.

27-43.

27. Curtiss, C.F. and J.O. Hirschfelder. "Integration of Stiff Equations." *Proceedings of the National Academy of Sciences of the United States of America,* vol. 38, no. 3, pp. 235-243.
28. Strikwerda, John. *Finite Difference Schemes and Partial Differential Equations.* 2nd ed., Society for Industrial Applied Mathematics, 2004.
29. Dahlquist, Germund. "Convergence and Stability in the Numerical Integration of Ordinary Differential Equations." *Mathematica Scandinavia,* vol. 4, 1956, pp. 33-35.
30. Lorenz, Edward. "Deterministic Nonperiodic Flow." *Journal of Atmospheric Sciences,* vol. 20, 1963, pp. 132-135.
31. Neri, F. *Lie Algebras and Canonical Integration.* University of Maryland, 1988.
32. Gao, Yingjie; Zhang, Jinhai and Zhenxing Yao. "Third-Order Symplectic Integration Method With Inverse Time Dispersion Transform for Long-Term Simulation." *Journal of Computational Physics,* vol. 314, 2016, pp. 436-449.
33. Verlet, Loup. "Computer Experiments on Classical Fluids 1. Thermodynamical Properties of Lennard-Jones Molecules." *Physical Review,* vol. 159, 1967, pp. 101.
34. Bagla, J. "Cosmological N-Body Simulation: Techniques, Scope and Status." *Ithaca,* 2004, http://arxiv.org/abs/astro-ph/0411043
35. Ruth, Ronald. "A Canonical Integration Technique." *Transactions on Nuclear Science,* vol. 30, no. 4, 1983, pp. 2669-2671.